EXTENDING URBAN SCALING THEORY BETWEEN AND WITHIN CITIES: ANALYSES OF INTER-CITY NETWORKS AND KINETIC EXCHANGE MODELING OF LOCAL INCOME INEQUALITY

Jacob J. Jackson
Department of Physics
Brown University

James Valles
Department of Physics
Advisor - Brown University

Chris Kempes
Advisor - Santa Fe Institute

Vicky Yang
Advisor - Santa Fe Institute

Elisa Heinrich Mora
Collaborator - Minerva Schools

May 1, 2020

ABSTRACT

Advances in Urban Science, particularly Urban Scaling Theory, have begun to uncover and explain urban dynamics shared by cities across time and place. This thesis extends Urban Scaling Theory to consider cities as non-isolated systems (cities interacting with other cities) of heterogeneous agents (non-uniform distributions of scaling behavior within cities). First, we analyze how cities' scaling properties are affected by their connectivity in inter-city networks. We find a significant effect on scaling behavior by inter-city interactions as measured by air traffic and presence of global firms. Second, we demonstrate how heterogeneous populations within cities scale differently across city size by characterizing income distributions across US Metropolitan Areas. We find that income inequality grows with city size. In order to understand this phenomenon, various agent-based Kinetic Exchange Models of Income and Wealth are tested in varying network structures to simulate the observed characteristics of income distributions across city size.

Contents

1 Literature Review & Introduction

1.1 Urban Scaling

It has been observed that many diverse processes of urbanization demonstrate very similar scaling behavior across city size: Urban indicators ranging from economic to social grow relative to city size in a surprisingly consistent and predictable way. In particular, many urban indicators ranging from GDP to patent production follow a power-law function of the population of a city, with a given property Y following the relation in Equation 1 [1]. These features have been found in urban locations ranging from modern Boston to Bangalore and even to prehistoric settlements in Central America [2, 1].

$$Y(N) = Y_0 N^{\beta} \tag{1}$$

Y represents a wide variety of features of a city, such as wages, GDP, patent production, crime, or pollution. For productive processes, it is consistently found that $\beta > 1$, generally in range of $[1.05, 1.25]$ [1]. Properties which follow Equation 1 with β in this range are said to exhibit superlinear scaling. An example of superlinear scaling of GDP in the United States is presented in Figure 1, and many other examples of superlinear scaling of urban features have been reported in Urban systems around the world and in various time periods [1, 3, 4, 2]. Alongside these superlinear productivity-related urban indicators, several urban

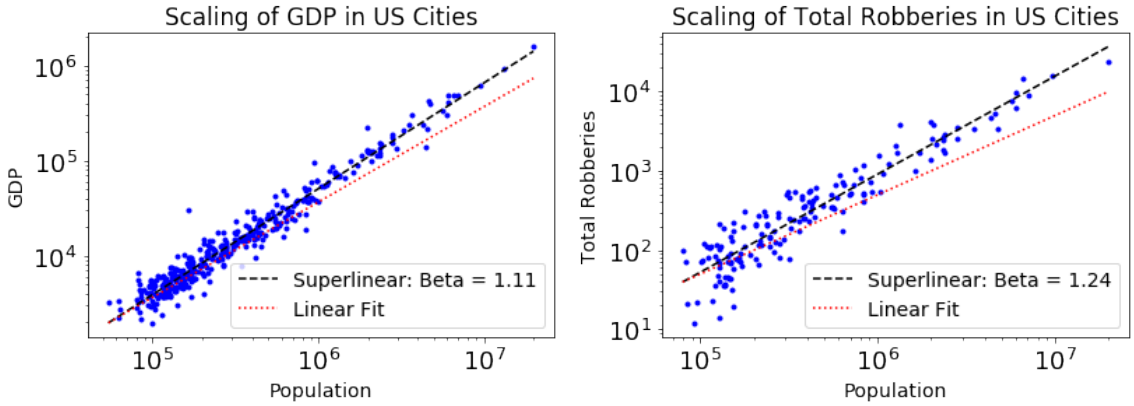

Figure (1) Examples of scaling in US cities for both GDP and crime (robberies). β from Equation 1 greater than 1, as in GDP and Crime here, demonstrates the superlinear growth seen in nearly all productive urban processes [1]. The red dotted lines in both figures demonstrate comparison to linear growth.

Scaling Exponent	Driving Force	Examples
Sublinear: $\beta \approx 1 - \delta$	Organization, efficiency	Road length, electric cable length, # gasoline stations
Superlinear: $\beta \approx 1 + \delta$	Social and economic interactions; possibly via densification of social networks	New patents, total wages, GDP, serious crimes, "supercreative" employment
Linear: $\beta \approx 1$	Individual maintenance	Housing, total employment, household water consumption

Table (1) Summary classification for scaling regimes as determined by scaling exponent β in Equation 1. Table adapted from [1]

indicators related to infrastructure are found to follow sublinear scaling: Equation 1 with approximately $\beta \in [0.70, 0.95]$ [1]. Another consistency in these scaling properties is the relation between superlinear and sublinear scaling relations: The two tend to deviate from linearity by the same amount. In other words, superlinear scaling occurs according to Equation 1 with $\beta = 1 + \delta$ and sublinear scaling occurs with $\beta = 1 - \delta$ for the same positive $\delta \in [0.05, 0.3]$. Table 1 lists these scaling regimes and corresponding examples of urban indicators demonstrating these scaling behaviors.

The self-consistency of this behaviour described by Equation 1 suggests common underlying urban dynamics. For comparison, these scaling laws have been found within biological systems as well, and arguably an underlying mechanism has been discovered [5]. Therefore, a brief divergence into biological scaling laws offers some insights into understanding urban scaling laws; this is especially true given that much of Urban Science has been directly inspired by work in biological scaling. Within biology, scaling behaviour has been found within metabolic rates of organisms.

Metabolic rate I, or "the rate at which organisms take up, transform, and expend energy and materials," [5] follows a power law of organisms' mass M: $I = I_0 M^{\frac{3}{4}}$. In other words, metabolic rates scale sublinearly in proportion to an organism's mass at a precisely measured exponent of $\frac{3}{4}$. This relation had been known for several decades without a clear explanation [6]. While still contested, a theory of scaling based on network interactions suggests an explanation. In this case, the networks at work are distribution networks within the organism: blood vessels, bronchial trees, plant vascular systems, and insect tracheal tubes, for example [6]. In their paper proposing this process, West et al. claim "Living things are sustained by the transport of materials through linear networks that branch to supply all parts of the organism" [6]. A mathematical derivation of the structure of the networks, based on simple assumptions about their function and form, arrive at a prediction of the metabolic scaling rate equation with the appropriate $\frac{3}{4}$ scaling exponent. The derivation centers around the structure of the distribution networks: They are understood to be fractal branching networks which most efficiently distribute materials throughout the organism's body. The power of this theory is also in its ability to indirectly explain other biological properties including mortality rates, population interactions, ecosystem processes, and more [5].

The success of scaling laws dependent on fundamental network-based mechanics evident in metabolic scaling laws research suggests a similar approach might be possible to understand observed scaling laws in cities. This is the motivation behind the leading hypothesis to explain the observed superlinear scaling in cities, led by researchers like Luis Bettencourt and Geoffrey West [7]. This hypothesis attempts to model urban scaling effects as the emergent behaviour of densifying social interaction networks as cities grow in size. One of the central ideas of this theory is stated directly in [7]: "socioeconomic outputs are proportional to local social interactions." This assertion effectively models urban features as outputs of emergent networks of social interactions occurring within any urban system. In other words, it proposes that a city is most fundamentally a dense system of social networks. Measures of urban outputs, ranging from crime to GDP to patent production, are thus the outputs of these social network interactions. In comparison, metabolic scaling theory proposed that observed metabolic scaling rates were the effect of scaling organism distribution networks, while urban scaling theory proposes urban scaling phenomenon are the effects of scaling (densifying) social interaction networks. Further relating these two theories is the observation that cities have their own distribution networks—roads, electrical wires, etc.—and their magnitude (e.g., total road area) follow sublinear scaling laws very similar to the sublinear scaling of metabolic rates. Thus, a network-based scaling theory akin to that applied to biological systems may be able to explain the consistent scaling behavior of cities described in Equation 1.

The central hypothesis of this theory is again that "socioeconomic outputs are proportional to local social interactions" [7]. Translating this idea into a mathematical model asserts that urban outputs Y are proportional to the rate of social interactions I:

$$Y \propto I \tag{2}$$

This leads to the very important question of how to model I, the rate of social interactions. To do so, we will reference some basic network theory, counting each edge in a social network as a social interaction. For a population with N people, a fully-connected network would have $\frac{N(N-1)}{2}$ edges (i.e., social connections), which for large N approaches $I \propto N^2$ edges. In a city of 10 million people, this would mean every person knows and/or interacts with 10 million other people, which is clearly unrealistic as most people only interact with a subset of the population in a large city. The other edge case is a network in which everybody interacts with the same fixed number of people n independent of city size, leading to a network with $\frac{n}{2}N$ edges, or $I \propto N^1$. This depicts the linear case, and is generally the null hypothesis against which the results exemplified in Figure 1 are compared. These two network examples present the boundary edge cases for what one might reasonably expect in modeling the city as a social network: $I \propto N^1$ and $I \propto N^2$, suggesting an expected social interaction rate somewhere in the middle: $I = N^\beta$ for $\beta \in [1, 2]$. After substituting this into Equation 2, which models urban indicators as proportional to these social network interactions (edges), this suggests $Y \propto N^\beta$. Simply adding a proportionality factor Y_0 to replace the proportionality with an equality derives Equation 1: $Y = Y_0 N^\beta$.

Equation 1 can be understood much more clearly using this idea: The N^β term counts the number of social interactions in the human network within the city, and the Y_0 term counts

the average socioeconomic output of those interactions. Lending strong evidence for this hypothesis, Schlapfer et al. [3] found that the number of mutual phone calls in Portugese cities scales consistently according to Equation 1 with a similar value of $1.00 < \beta < 1.25$ that models most socioeconomic properties. This study is profound for verifying this theory in that it is explicitly measuring the N^β term as social interactions and results are rather precisely consistent with what is expected given this theory of urban scaling of urban social networks. This lends strong evidence to the hypothesis that urban outputs—in particular, the related superlinear scaling of diverse properties ranging from crime to personal income—can in essence be understood as the outputs of complex human interaction networks which densify with city size.

1.2 Urban Scaling Deviations

Urban scaling theory not only provides a powerful theoretical framework for understanding urban systems holistically, it also provides a new set of measurements for urban indicators: the Scale-Adjusted Metropolitan Indicator (SAMI), which is described in this section and used in new analyses done in Chapter 2. The SAMI is meant to replace per-capita metrics for cross-comparison of indicators like crime rates or GDP between cities.

The SAMI is defined as [8]:

$$\xi_i = \log \frac{Y_i}{Y_0 N_i^\beta} \tag{3}$$

in which Y_i is the measured urban indicator for city i (e.g. crime incidents in New York) and $Y_0 N_i^\beta$ is Equation 1 (with Y_0 and β measured from the urban system, e.g. all U.S. cities) evaluated at the population of city i. Thus, the ratio $\frac{Y_i}{Y_0 N_i^\beta}$ is a dimensionless unit and the denominator can be understood as $Y(N_i)$, the expected value based only on the city's population using Equation 1. In a scaling plot like Figure 1, $Y(N_i)$ corresponds to the point on the dotted black line at the city's population N_i.

The key difference between SAMI and per-capita metrics is that the SAMI metric is scale-adjusted, meaning that it accounts for non-linear scaling (agglomeration) effects in cities. It is best to understand this by first demonstrating how per-capita metrics implicitly assume linear scaling in cross-comparisons between cities. Take an example of per-capita crime incidents in two cities. A common metric for cross-comparison would be to compare their per-capita crime incidences:

$$\frac{Y_A}{N_A} - \frac{Y_B}{N_B} \tag{4}$$

in which Y_A (Y_B) is the number of crime incidents in City A (City B) and N_A (N_B) is the population of City A (City B). As figures like Figure 1 have consistently demonstrated, crime incidents scale superlinearly ($\beta > 1$ in Equation 1) with population and can be approximately predicted by Equation 1. Therefore this difference of per-capita metrics can be re-expressed using Equation 1:

$$\frac{Y_A}{N_A} - \frac{Y_B}{N_B} = \frac{Y_0 N_A^\beta + \delta_A}{N_A} - \frac{Y_0 N_B^\beta + \delta_B}{N_B} \tag{5}$$

$$= Y_0(N_A^{\beta-1} - N_A^{\beta-1}) + (\frac{\delta_A}{N_A} - \frac{\delta_B}{N_B}) \tag{6}$$

Suppose City A is New York, with a metro area population of about 20,000,000, and City B is Santa Fe, with a metro area population of about 150,000. In this case, the first term in Equation 6 would dominate over the second term which actually contains the δ terms which describe how a city differs from a standard city of its size. In effect, per-capita metrics in cities are dominated by the size of the city rather than by what makes the city different from other cities.

Therefore, to remove this effect, the SAMI adjusts for scale by instead analyzing $\frac{Y_i}{N_i^\beta}$ which removes the superlinear scaling component N^β in Y. In the full SAMI (Equation 3), $\frac{Y_i}{N_i^\beta}$ is the only variable component for each city i. The Y_0 and $\log$ allow the SAMI to be understood as a residual in log space: $\log(Y_i) - \log(Y_0 N_i^\beta)$. A positive SAMI means a city is above the trend-line, or can be said to "overperform." Likewise, a negative SAMI indicates a city is below the expected trend-line or can be said to "underperform."

It is important to clearly define how to interpret the SAMI of a given city. Most simply, the SAMI provides a quantitative answer to the question: To what extent does the activity in this city (being measured through the indicator, e.g. income) fall above or below the amount that would be expected of a "typical" city of its size? However, in reality there is no such "typical" city, rather an aggregate/interpolated expected behavior derived from other cities of a similar size (using Equation 1). Therefore, to refer to a city with negative SAMI as "underperforming" is not necessarily making a critical statement about the functioning of that city. Rather, it is only observing that that city does not produce as much income, crime, patents, or other urban indicator as do most cities of that size.

The power of this is to provide a scale-adjusted metric for a city's performance relative to the total urban system. For example, the largest SAMI for income of US cities is Bridgeport, CT, a small city with a metro population of under a million. This is likely due to its strong ties with nearby New York City. The San Francisco Metropolitan Statistical Area (MSA), the 7th largest in the US, has the 10th largest income SAMI, likely due to its centrality in the technology economy. In contrast, the Los Angeles MSA, the 2nd largest MSA, has an income SAMI that is among the lowest in the country. These examples demonstrate the size-independent analysis that SAMIs allow for any city, providing more meaningful characteristics of a city as compared to the full urban system.

SAMIs also allow for a comparison of the deviations of urban indicators in cities. In their paper originally defining the SAMI, Bettencourt, et al. explored the cross-correlations of SAMIs of income, patents, and crime [8]. Their results are shown in Figure 2, sub-figures A, B, and C. They find a positive correlation between income and patents, and a weaker negative correlation between violent crime and both patents and income. Bettencourt, et al. also investigated spatial correlations of SAMIs. Figure 2, sub-figure D shows a small degree

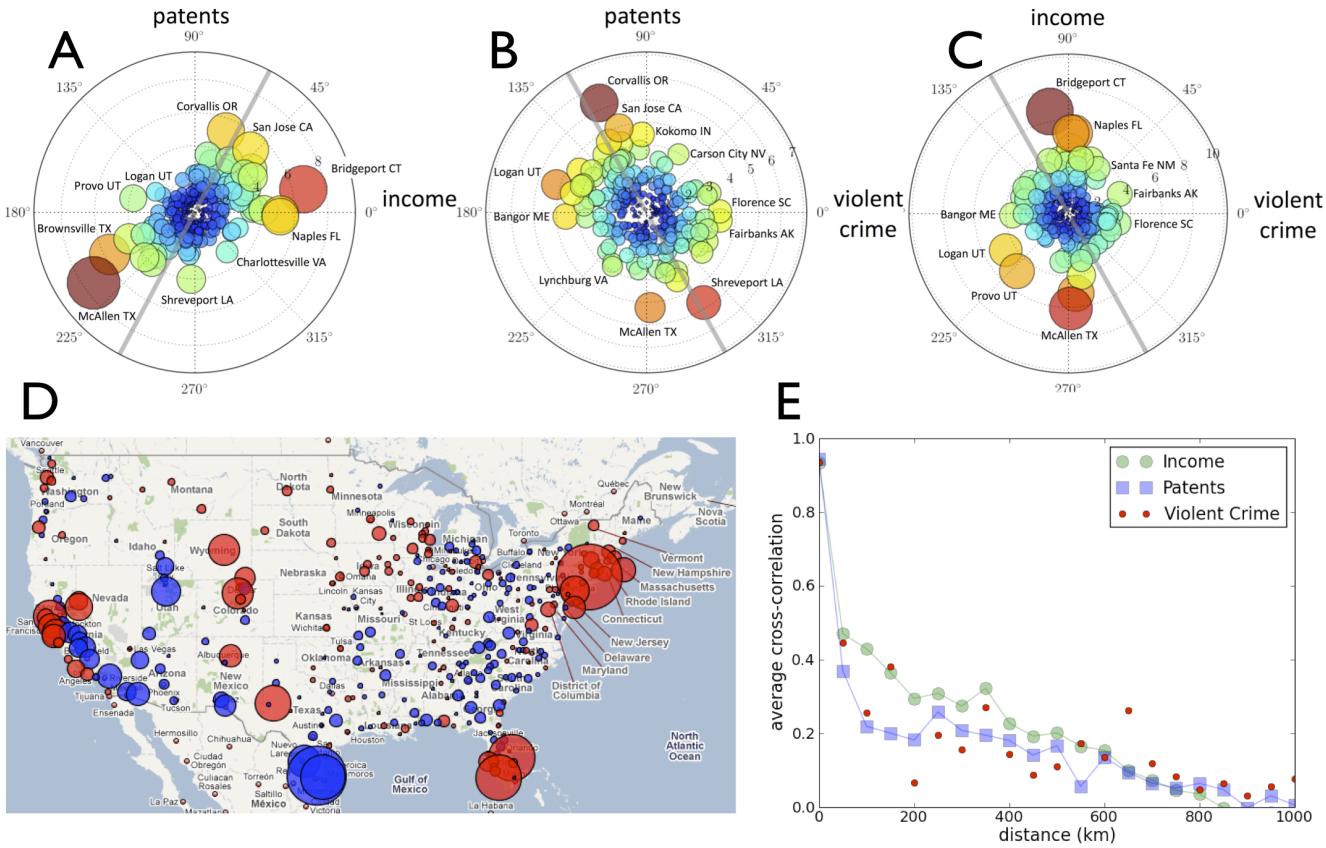

Figure (2) **Analyzing cross-correlations of Scale-Adjusted Metropolitan Indicators (SAMIs)** *(Figure originally from [8])*
A) cross-correlation between SAMIs for income and SAMIs for patents for all US cities, shown in a polar plot in which the angle represents the ratio between the two SAMIs. The size and color of the circles both represent the size of the SAMIs. A trendline is shown, with $R^2 = 0.20$
B) similar plot for patent SAMIs versus violent crime SAMIs with $R^2 = 0.12$
C) similar plot for income SAMIs versus violent crime SAMIs with $R^2 = 0.05$
D) Map of spatial distribution of SAMIs for income. Red (blue) dots represent deviations above (below) expectation for city size. Similar to the A, B, and C, the size of the circle represents the magnitude of the SAMI. Note that the largest SAMI is Bridgeport, CT.
E) Relationship between separation distance and average spatial cross-correlation, demonstrating a notable but small degree of short-range spatial correlation.

of spatial correlation of income across US cities. Sub-figure E more clearly demonstrates this correlation across distance [8]. Additionally, the study finds that this spatial correlation has diminished over time, suggesting weakening homogenizing effects within spatial regions over time.

1.3 Inter-City Networks and Global Cities

Ample research makes clear that the world is becoming increasingly global [9, 10, 11] alongside becoming increasingly urban [12]. As the goal of Chapter 2 is to explore the relationship between these two trending characteristics, this review section provides background on relevant research on the implications of cities' connectivity to inter-city networks. These inter-city networks can be social and institutional networks which foster interactions between cities. The two precise forms of inter-city networks analyzed in this study are air traffic networks and the World City Network. While the former is simpler, the latter is important to review, both for understanding its use in Chapter 2 and for reviewing some of the Geography literature concerned with global cities and inter-city networks. Then, two existing theories of inter-urban network effects are reviewed.

1.3.1 Defining and Measuring Inter-City Networks

Many scholars from varying disciplines have developed different theoretical frameworks and definitions of inter-city networks [11, 13, 14]. While these varying definitions serve theoretical purposes in different disciplines, many lack a precise measurable definition. PJ Taylor et al. constructed the World City Network precisely to fill that gap [15]. Many measurements of inter-city networks used in research are infrastructural and focused on the flow of individuals: air traffic, migration patterns, electric communication infrastructure, etc. These are of course important and relevant to inter-city networks as defined by Taylor et al., but are merely the supportive infrastructure for inter-city interactions and do not themselves define inter-city interactions. Instead, the goal of measuring the inter-city network is to construct a social network in which cities themselves are nodes that can be treated as social actors. Of course, cities do not act purely collectively and instead only respond to emergent behavior patterns of agents within themselves (i.e., policymakers, voters, business leaders, cultural figures, etc.). Thus, the World City Network is constructed with a sub-nodal level: global firms. Global firms can be considered social actors within the network of cities but act, to a large extent, in response to their environment; in other words, global firms are agents within and across cities that construct and mediate the inter-city network while cities themselves are the "vital enabling environs" [15]. The choice to measure global firms is made based on research demonstrating the importance of global firms in leading processes of globalization within cities [11], specifically advanced producer services firms which do highly specialized work such as law, accounting, or engineering. Thus, the presence of 100 top global advanced producer service firms in 315 cities worldwide is qualitatively assessed and given a rating from 0 (no presence) to 5 (firm headquarters). This constructs a network for each firm which can be combined to construct the full World City Network. A city's centrality within that network can then be measured to describe the Connectivity of a city in the inter-city network, defining the degree to which a city interacts with other cities.

The theoretical distinction between an infrastructural metric like air travel networks and the World City Network is a subtle but important one which can best be understood in relation to theories of agglomeration economies. Agglomeration economies are the economic framework for understanding the superlinear scaling effects described in Section 1.1 and

frequently referenced within the urban scaling literature as well [16]. Puga describes three primary mechanisms of agglomeration economies: sharing, learning, and matching [17]. While these agglomeration economies are generally understood to exist within cities, many also believe them to play a role in the inter-city network [18, 19], and thus it is important to measure sharing, matching, and learning across the inter-city network. Sharing is the process by which large networks share resources, infrastructure, and people [17]. Metrics like travel patterns are understood to measure the process of sharing [18]. In contrast, it can be understood that the World City Network measures learning and matching. Learning is the process by which knowledge is created and distributed, and global firms are a clear example of learning within the inter-city network given the accumulation of knowledge across firm branches in different cities distributed across the firm network. Matching is the process by which people are matched with opportunities most optimal for them, generally through labor sourcing [17]. By relocating staff between firm locations across cities, global firms could play a role in contributing to inter-city matching, though it is less apparent that this would be a significant effect as compared to learning.

By relating the different metrics to theoretical understandings of agglomeration economies applied to inter-city networks, this provides a clearer picture of the metrics important to measuring inter-city networks, how they are to be understood, and why they are chosen. It is also important to note here that the World City Network is constructed as a measure of *economic* inter-city connectivity.

These inter-city network measurements provide descriptive characteristics of inter-city networks, laying the groundwork for the perhaps more important work of developing predictive theories about the effects of inter-city networks. Thus, some relevant theories are discussed here from different disciplines: Borrowed size, and urban gravity models. There are many more theories one might investigate, but these two are chosen based on their relevance to the original work conducted in this thesis.

1.3.2 Borrowed Size Theory & Urban Gravity Models

Originally theorized by William Alonso in 1973 [20], the theory of borrowed size proposes that a city with a large flux of people from outside of the city may exhibit more metropolitan functions than would be expected based solely on its internal population. Alonso and later Burger et al. [19] theorize an effective city population, referred to as "population ootential," that includes local residents in addition to people not living in the city who interact significantly with the city. A simple example of population potential would be redefining London's population to include a proportion of the population of nearby Cambridge; while residents of Cambridge are not considered residents of London, they are very likely to have strong and significantly productive interactions with the resident population of London due to their close proximity as well as the academic, cultural, and institutional ties between the two cities. Population potential defined in a global sense could additionally include cross-city business partnerships, tourists who frequently fly or take a train into the city, or perhaps simply call people in the city.

Burger et al. made the important contribution of analyzing Population Potential beyond just regional effects to also include added population potential from global networks (e.g. people flying in and out of a city) [19]. Meijers et al. continued this work, conducting a study of the relationship between global or regional connectivity and the presence of metropolitan functions in European cities [18]. Global/regional inter-city connectivity was measured explicitly as population potential via data on worldwide air, rail, and marine networks. Metropolitan functions measured were international institutions, science, firms, culture, and sports. In their study, they found that while city size is still the dominant factor in determining the level of metropolitan functions in a city, network connectivity does play a significant role as well. In particular their study suggests that, after other variables are accounted for, about 70% of remaining variations in metropolitan functions can be described by local population, while the other 30% is attributable to global network connectivity [18]. This corroborates existing understanding that local size is still the dominant factor in a city, however global networks are beginning to have non-negligible effects that are not explained by local size alone. Additionally, this study found that global network connectivity has a more significantly positive effect on level of metropolitan functions than regional networks. This suggests that borrowed size effects are less dependent on proximity and more generally suggests that inter-city networks are less bound by spatial proximity than they are by cities' connectedness in inter-city network infrastructure like the air, rail, and marine networks studied in [18].

Urban gravity models vary widely, and are mostly used to model "urban flow:" the movement of people, materials, and information [21]. The traditional gravity model describes either strength or probability of interaction between two cities according to [22]:

$$P_{ij} = \frac{P_i P_j}{c_{ij}^{\eta}} \tag{7}$$

in which c_{ij} is the distance (or other cost function) between cities i and j, η is a scaling exponent, and P_i (P_j) is a "weight" of city i (j), often set by city's population or some other metric on centrality or popularity [21, 22].

In relation to inter-city networks, Gravity models of the form in Equation 7 are often used to model Urban flows of people [21] and corresponding urban growth and development [21, 23]. The most simplest of these take a city's "weight" to be its population and the cost function to be the geographic distance between cities [21]. This is a very regional interpretation of inter-city interactions by its emphasis on spatially-mediated interactions. It allows for a widely generalizable model of inter-urban dynamics that has been used to model a variety of inter-urban dynamics [21]. Like borrowed size theory, urban gravity models provide a valuable method of understanding inter-city interactions and their effects in cities, but little work has been done to understand the relationship between inter-city interactions and specifically urban scaling behavior.

1.4 Intra-Urban Networks and the Scaling of Urban Inequalities

The second half of the original work in this thesis, in Chapter 3, pivots from inter-urban networks (networks of cities interacting with cities) to intra-urban networks, the interaction

networks *within* a single city that represent how different individuals and groups of individuals in that city experience and gain from their connections within that city differently. In other words, Chapter 3 seeks to uncover inequalities within urban scaling phenomena through the lens of intra-urban networks: As agglomeration effects bring super-linear aggregate growth of things like income, patents, and crime in larger cities, how do different sub-populations experience this growth differently? What is the relationship between these inequalities and the intra-urban network structure? In this subsection, various theories and analyses from existing research related to these questions are reviewed.

1.4.1 Measurements of Intra-Urban Interaction Networks

A central hypothesis of urban scaling theory is that urban outputs are fundamentally outputs from human interactions and that these interactions scale in number with city size [7]. A study by Schlaepfer et al. has attempted to empirically test this theory [3], and in doing so has produced a powerful, almost direct measurement of intra-urban interaction networks. By analyzing phone calls placed within cities in Portugal and the United Kingdom, the study found that the total number of interactions and the number of contacts per person scaled superlinearly with city size at nearly the same rate as many urban indicators, according to Equation 1 with $\beta \approx 1.1$, and within 95% confidence intervals for nearly all measures of interaction rates $\beta > 1$. This result is unique in its ability to directly test a core hypothesis of urban scaling as a social interaction network theory. The findings align quite precisely with the theoretical expectations. This study importantly also begins to explore questions about the network structure of social interactions within a city.

The data on phone calls analyzed was used to reconstruct a partial interaction network for each city. Using this reconstructed interaction network as a proxy for the true social interaction network within the cities, Schlaepfer et al. were able to almost directly measure the intra-urban interaction networks at the microscopic (individual) level to develop an understanding of the structure of these networks and how they change across city size. This analysis showed that the probability that two contacts of the same individual are also connected with each other is nearly the same across city size (around 25%) [3], as measured through the clustering coefficient of the social network. Taken with the observation that total interaction rates scale superlinearly across city size, this suggests that an individual's network becomes larger in a larger city, but is approximately equally clustered (or "tight-knit") in any city size. Furthermore, the study measured the probability distributions of interaction rates within the city, showing that they were best approximated as log-normal or skewed log-normal probability distribution functions (PDFs). These PDFs are shown here in Figure 3, and are perhaps the most direct measurement yet of the intra-urban interaction networks that Chapter 3 seeks to uncover.

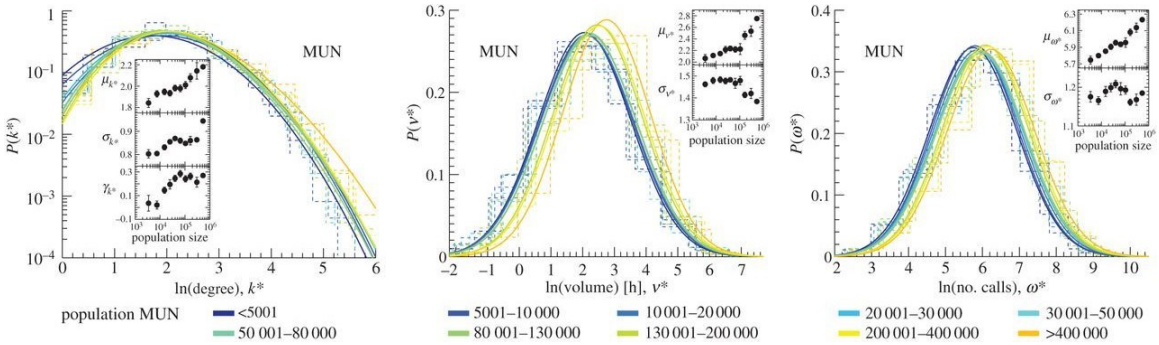

Figure (3) *(Figure, originally from [3])*
From left to right: Probability distribution functions in an individual city (averaged over the many cities in the dataset) for (left to right): node degree, call volume (time spent on calls), and number of calls. In the inset sub-figures, μ, σ, and γ denote the mean, standard deviation, and skewness of the distributions.

1.4.2 Urban Allometry & Economic Distributional Implications

The ultimate goal of understanding the structure of intra-urban networks through this work is to understand its relationship to distributional characteristics—that is, how urban indicators like income are distributed across individuals within the city—and the patterns of urban inequalities they describe. A pair of studies by S. Sarker et al. [24, 25] begins to explore this idea by analyzing distributions of incomes in cities in Australia and the United States. Their most important finding, shown here in Figure 4, was that different income groups show different scaling behavior across city size: Low-income groups scale sub-linearly or linearly, middle-income groups scale linearly, and the highest-income groups scale super-linearly (with β much higher than in the aggregate). In effect, this means there are increasingly more rich (high-income) people and less poor (low-income) people per-capita in larger cities. Sarkar refers to this phenomenon as an example of "urban allometry:" different sub-groups within cities scaling differently across city size [24]. Urban allometry of this form has important implications for the socioeconomic considerations of how cities are measured and understood, and most importantly the policies that are derived from those measurements and understandings. Therefore, issues of *distribution* of agglomeration effects in cities should be seriously considered by the urban scaling literature, which can greatly compliment and add to existing research on cities' role in growing inequalities.

There is ample existing research on the characteristics of income inequality within cities. All studies reviewed find, at least to some degree, that larger cities exhibit larger income and wage inequality [26, 27, 28]. These studies included both longitudinal (across time) and cross-sectional (across city-size at one time) analyses, all of which showed the same clear trend: Larger cities are more economically unequal. In fact, one of the most expansive longitudinal studies found that these inequalities have been growing at an accelerating rate since the late 20th century [28]. In other words, not only are larger cities more unequal, but this effect of urban inequality has been rapidly increasing at a time when the world is urbanizing at unprecedented rates. Many economists attribute this phenomenon to various

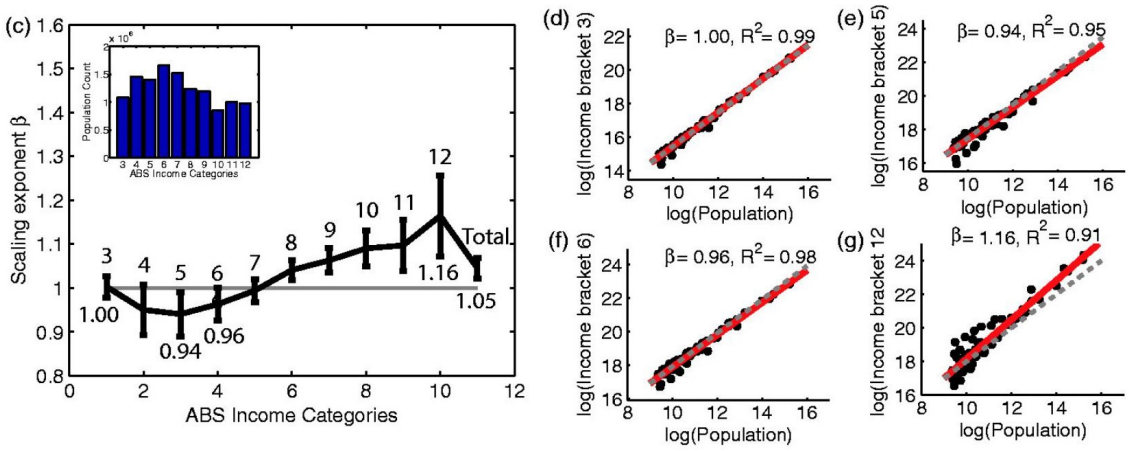

Figure (4) *(Figure, originally from [24])*
Scaling of income categories in Australian cities. Left plot shows scaling exponents β (as in Equation 1) for lower to higher income categories, demonstrating linear/sublinear growth for low-income groups and superlinear growth for high-income groups. Right plots are the scaling plots of income subgroups.

dynamics of labor migration, where higher- and lower-skilled workers are found and how their skill is valued differently [26]. A common proposition is that much of the observed income inequality growing within and between cities is attributed to both a disproportionate concentration of high-skilled workers in larger cities and significant within-skill-group income inequalities in those larger cities [28]. The study by Baum et al. demonstrated this empirically [28]. This study more generally concluded that their results "suggest an important role for agglomeration economies in generating changes in the wage structure." Another study conjectured that "everything that promotes urbanisation and, more generally, the growth of cities also has direct impacts on income inequality across individuals" [26].

1.4.3 Relationship Between Intra-Urban Networks and the Scaling of Urban Inequalities

Some studies have moved closer toward connecting urban income inequalities within cities to the networks of interaction within those cities. For example, one of the aforementioned studies which found that larger cities are more unequal also found that this inequality partially mapped onto spatial segregation [25]. This is especially noteworthy given existing research on the 'neighborhood effect,' the "self-reinforcing effects of economic, health, crime, and education inequalities" [25] that are often rooted in spatial organization within cities [29].

Eagle et al. went perhaps the furthest in drawing the link between economic indicators and social networks [30]. In a study using the same type of data on mobile phone networks as in the study reviewed earlier in Section 1.4.1 [3], Eagle et al. measure the relationship between network diversity and economic development at the community level [30]. Network diversity means the diversity of contacts one has; an individual who interacts with people spanning many social clusters has a more diverse network. Comparing the mobile phone

data with measures of economic development and well-being in UK communities, Eagle et al. found a strong correlation between the diversity of an individual's network and the economic well-being of the community in which they lived. While cautioning that this study did not conduct a causal analysis, the resulting correlation can be interpreted in different ways: *Individuals* with more diverse networks may have greater access to socioeconomic opportunities, *communities* of people with diverse networks may have greater access to socioeconomic opportunities, or the reverse effect is true: individuals/communities with greater existing socioeconomic opportunities are or become more diversely connected [30]. Whichever direction the causality may go, evidence suggests it applies both to communities and individuals. Eagle et al. review research that demonstrates individuals tend to benefit from having more diverse network [30]. As for the relationship between a community's network diversity and economic well-being, current theories of Urban Science within the scaling literature believe quite explicitly that a stronger-connected community should see larger agglomeration benefits to economic indicators [7], as most theories of agglomeration economies would suggest [16]. While it is not equivalent, it is worth noting here that several economists have argued that economic equality has a positive relationship with overall economic growth (for example, at the national level), suggesting that if a community with a more diverse network were consequently more economically equal, then it would experience greater economic growth and well-being [31]. However, this draws many links which are as-of yet unproven (namely the relationship between network interconnectedness and economic equality).

Collectively, these studies provide some evidence to suggest a relationship between intra-urban network structure and urban economic distributional effects (allometry). As motivated by this evidence and the questions posed by this existing body of research on the relationship between urban networks and urban inequalities, Chapter 3 of this thesis presents a new way of understanding and modeling these inequalities by merging theories and methods from Urban Scaling, Economics, Econophysics, and Network Theory. First, one of these methods is reviewed in the following section.

1.5 Kinetic Exchange Models

Many quantitative scientists have applied tools from statistical physics to understand a variety of topics in social sciences. Statistical physics has already been used to describe aspects of cities [32], elections [33], and belief change [34], for example. This application of statistical physics to social systems is no new idea. Ludwig Boltzmann, known as the father of statistical mechanics, had the same ideas when he developed the science, saying [35]:

> "This opens a broad perspective, if we do not only think of mechanical objects. Let's consider to apply this method to the statistics of living beings, society, sociology and so forth."

Econophysics is a field of physicists and economists who have followed this idea by applying various physics tools to understand economic phenomena [36]. For example, the theory of

potential games combines information theory with statistical physics to create and extend models of bounded rationality in economic systems [37]. Some of the better-known ideas from Econophysics are kinetic exchange models of markets, referred to sometimes as Kinetic Wealth Exchange Models, and referred to here as Kinetic Exchange Models. Kinetic Exchange Models are a key component to the urban income modeling used in section 3.2 and are reviewed in this section.

Kinetic Exchange Models (KEMs) are an attempt to model wealth exchange in economic systems using very basic ideas from analogy to kinetic exchanges between colliding particles in a gas. The most simple KEM is to take the well-understood problem of a gas in a box and replace particles and kinetic energy with people and wealth, respectively. Assuming energy is conserved, the energy of two interacting particles in a box would change according to

$$\begin{aligned} E_i(t + \Delta t) &= E_i(t) + \Delta E \\ E_j(t + \Delta t) &= E_j(t) - \Delta E \end{aligned} \tag{8}$$

for some exchanged energy ΔE. The KEM version of this equation is then

$$\begin{aligned} w_i(t + \Delta t) &= w_i(t) + \Delta w \\ w_j(t + \Delta t) &= w_j(t) - \Delta w \end{aligned} \tag{9}$$

where w_i is the wealth of person i, exactly analogous to the energy of particle i. Part of this analogy rests on principles of conservation: Just as energy is the conserved quantity in the physical case, wealth is the conserved quantity in the market case [38]. It is simple to demonstrate that, in the particle in a box problem described in Equation 8, the gas particles' energy will have a Boltzmann-Gibbs distribution [38]. Thus, the KEM model suggests that if people exchange money approximately the way particles exchange kinetic energy, real wealth distributions will appear approximately as a Boltzmann-Gibbs distribution. Mathematically, this is stating that in the model, w_i has the same distribution as E_i by the fact that the they follow the same mathematical definition. Indeed, measured wealth distributions have been found to be quite similar to a Boltzmann-Gibbs distribution [38] for the bulk of populations. However, this approximation fails for higher-income groups. An example of this is demonstrated using income data aggregated across all US Metropolitan Statistical Areas (MSAs), seen in the orange fit line in Figure 5.

The key empirical observation that deviates from the Boltzmann-Gibbs distribution is something Vilfredo Pareto discovered in 1964: a fat tail in the wealth distributions for the highest incomes, seen in many different economies [39]. This is again demonstrated in Figure 5. This suggests, perhaps unsurprisingly, that this most basic KEM which treats people exchanging wealth *exactly* like particles exchanging energy is not a very accurate model. However, further work on KEMs has tried to develop upon this basic analogy to create a model of wealth exchange which still relies only on very basic assumptions but can produce realistic wealth or income distributions.

In order to devise a similar model that can describe both the Boltzmann-Gibbs bulk and Pareto tail, the KEM can be generalized. We still consider particles in a box interacting randomly with perfect conservation of energy, but instead propose some consistency in their wealth/energy exchanges. This generalization takes the same form as Equation 9,

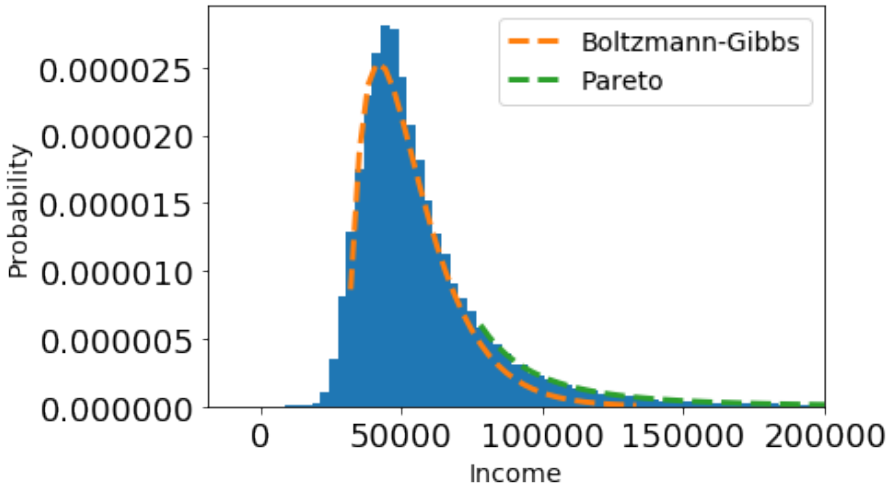

Figure (5) Income distribution produced from aggregated income data across all US Metropolitan Statistical Areas. The two fit lines demonstrate the two sections of the distribution most frequently identified in Econophysics studies: a Boltzmann-Gibbs distribution describing the lower and middle sections, often the large majority of population; and a Pareto distribution describing the fat tail for the highest incomes.

but the Δw term is a known function Δw_{ij}, often of w_i and w_j. The definition of Δw_{ij} provides a complete definition for a KEM. Once Δw_{ij} is defined, the model might be solvable analytically, but nearly all must instead be simulated by randomly choosing agents i and j to interact, updating their wealths between time t and $t+1$ according to:

$$w_i(t+1) = w_i(t) + \Delta w_{ij} \tag{10}$$

$$w_j(t+1) = w_j(t) - \Delta w_{ij} \tag{11}$$

Some examples of functions for Δw_{ij} are listed and explained below [40, 38]:

$$\Delta w_{ij} = \pm \Delta w \tag{12}$$

$$\Delta w_{ij} = \gamma w_j - \gamma w_i \tag{13}$$

$$\Delta w_{ij} = \epsilon w_j - (1-\epsilon) w_i \tag{14}$$

Equation 12 is an additive exchange KEM, in which a fixed amount (e.g. \$10) is exchange in either direction between two agents whenever they interact. Equation 13 is a multiplicative exchange KEM, in which a fixed fraction γ of each agent's wealth is exchanged between two agents when they interact. Lastly, Equation 14 is a stochastic exchange KEM, in which ϵ is a random number between 0 and 1 generated at every interaction. This characterizes a random redistribution of combined wealth of agent i and j during interaction. Several of these models produce distributions that get closer to empirical wealth distributions [38]. These models can also be built upon each other. One such model, later used in this thesis' original work, is presented in the following section.

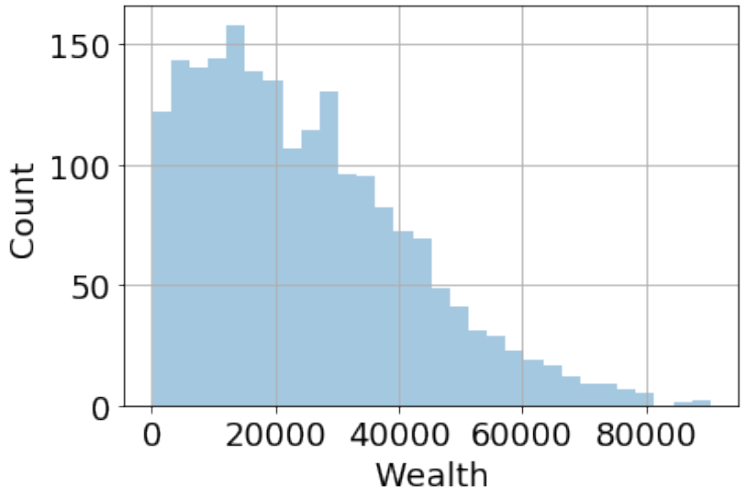

Figure (6) A resulting wealth distribution from simulating the KEM defined by Equation 15, run with 2000 agents.

1.5.1 Kinetic Exchange Model with Stochastic Exchange and Distributed Savings Rates

One KEM which has been shown to produce both the Gamma bulk and Pareto tail of empirical wealth distributions is one examined by Chakraborti [41] and Angle [42], described by defining Δw in Equation 9 as

$$\Delta w_{ij} = -(1-\lambda_i)w_i + \epsilon((1-\lambda_i)w_i + (1-\lambda_j)w_j) \tag{15}$$

This KEM can equivalently be described by writing

$$w_j(t+1) = \lambda_j w_j(t) + \epsilon((1-\lambda_j)w_j(t) + (1-\lambda_i)w_i(t))$$
$$w_i(t+1) = \lambda_i w_i(t) + \overline{\epsilon}((1-\lambda_j)w_j(t) + (1-\lambda_i)w_i(t))$$

where ϵ is a random number in $[0,1]$, $\overline{\epsilon} = 1-\epsilon$.

This KEM combines the multiplicative KEM (Equation 13) and the stochastic exchange KEM (Equation 14). Each agent i exchanges $(1-\lambda_i)$ of their wealth (equivalently saving λ of their wealth) at each interaction, then a stochastic fraction ϵ of the sum $(1-\lambda_i)w_i+(1-\lambda_j)w_j$ is taken by agent i. The final component of this KEM is the distributed savings rates λ_i. In this KEM, each agent has a different savings rate randomly chosen from an inverse power-law distribution, with very few agents having very high savings rates [42]. An example wealth distribution produced from running a KEM process according to Equation 15 is shown in Figure 6.

2 Uncovering and Characterizing Inter-Urban Network Effects Using Scale-Adjusted Metropolitan Indicators

As stated above in Section 1.1, urban scaling theory [7] assumes that socioeconomic outputs are proportional only to "local" social interactions [7], neglecting the vast human

networks that are not bound within the city but instead occur at an inter-city level. These social networks consist of everything from tourism to business connections and have been measured through indicators such as air-flight traffic, internet links, trade flows, global business ties, and more. These inter-urban network interactions have already been shown in previous studies to be significantly correlated with indicators of urban functions [18, 19].

This chapter has two objectives centering on inter-urban network effects in cities: First, to use urban scaling theory to uncover and investigate these inter-urban network effects; and second, to consider extensions of the urban ucaling model which consider both local interactions and semi-local interactions (also referred to as inter-urban network interactions). This extended model maintains the hypothesis that cities are the emergent behavior of human interaction networks while also incorporating semi-local interactions arising from inter-urban networks.

Accordingly, the chapter begins with an investigation into the effects of inter-urban network interactions on properties of cities. Significant positive correlations are found between economic (urban network) connectivity and economic outputs of a city, demonstrating a significant and consistent effect of inter-urban network interactions on urban scaling features. Based on this observation, two models are then proposed to incorporate semi-local interactions into a more comprehensive urban scaling theory.

First, inspired by previous work and ideas from Alonso [20] and later Burger et al. [19], a theory of "Borrowed Size" is proposed. In this Borrowed Size model, the fundamental mechanisms and assumptions of urban scaling are retained, but the population of a city is redefined as an effective population which includes both local residents and individuals outside of the city confines who interact significantly with residents of the city (in other words, a "semi-local" population). Formalizing this Borrowed Size theory and testing it against data from cities in various European countries, we find that this model can provide a slightly better fit to empirical observations than the traditional urban scaling model.

Next, the Urban Network Production Model is presented, which includes urban network interactions of three forms: Local interactions, as in Equation 1; Visiting interactions, where people physically travel to another city; and Institutional interactions, where institutions (e.g. global firms, universities, etc.) form strong direct links across cities. This model produces a better fit to empirical observations than both the borrowed size model and the urban scaling model (Equation 1). This suggests that the Urban Network Production Model might provide a more representative and comprehensive understanding of the universal phenomena of cities when understood as the outcomes of emergent human interaction networks that are both local and semi-local.

2.1 Relating Scaling Deviations With Connectivity in the Inter-Urban Network

Previous work by Bettencourt et al. has analyzed the deviations from urban scaling expectations observed in US cities as measured using the Scale-Adjusted Metropolitan Indicator (SAMI), which effectively measures the scatter around the power-law fit line in figures like Figure 1 and is defined in Equation 3 [8]. The methodology, ideas, and key results from

this study are summarized in section 1.2. Their study presumes that these SAMI deviations are "truly local measures of a city's organization and dynamics."[8] They measured cross-correlations of SAMIs to find only small regional effects that have been diminishing over time [8]. However, other studies outside of the urban scaling literature have suggested that global effects can be more significant than regional effects [19, 18]. Section 1.3 reviews further existing research on inter-urban networks and their effects in cities.

The goal of the study in this section is to investigate whether inter-urban network effects have a significant and consistent effect on deviations from scaling behavior. This can also be understood as an attempt to demonstrate that deviations from scaling predictions are not purely random statistics but can be understood in some part as the results of inter-urban network interactions affecting cities in a significant and consistent manner. To demonstrate this, we analyze two metrics for connectivity in the inter-urban network (i.e., the degree to which a city interacts with people and institutions in other cities): the presence of global firms as measured through the World City Network, and global air traffic networks. Both measures of connectivity in the inter-urban network are compared to various metropolitan indicators for cities across Europe and the US, using a cross-correlation study of SAMI deviations similar to that in [8] and reviewed in Section 1.2.

2.1.1 Data & Methods

Data on population, GDP, patents, and unemployment at the city-level were collected from Eurostat and the Organisation for Economic Co-operation and Development (OECD) for several hundred cities in Europe and many OECD countries. To quantify social inter-urban network interactions, data from Eurostat is used to measure the number of people flying into all airports within a given city. To quantify economic inter-urban network interactions, data is taken from PJ Taylor's World City Network in the years 2000-2005 [15]. This data measures the presence of global advanced producer service firms, and is a standard across studies of global cities [9, 43, 44]. The choice of these types of global firms as a metric for economic inter-urban network interactions is based on the hypothesis of Saskia Sassen that global advanced producer service firms are one of the central indicators and drivers of a global city [11].

PJ Taylor's World City Network analyzes 100 top global firms in 315 cities worldwide in the year 2000, assessing the presence of each firm f in city i with a metric v_{ij} from 0 (no presence) to 5 (central headquarters) [15]. Given this dataset, 3 methods are used to calculate the economic connectivity of a city: Symmetric, asymmetric, and isolated. Each produces a Connectivity measure C_i of how embedded city i is in the inter-city network of global firms.

Symmetric Connectivity measures how connected a city is to other cities via co-presence of firms, giving equal weighting to 2 connected cities, independent of which has larger presence. This is calculated below in Equation16

$$C_i^{Symmetric} = \sum_f \sum_j v_{fi} s v_{fj} \tag{16}$$

Figure (7) Scaling behavior of the three connectivity metrics derived from the World City Network database [15].

Asymmetric Connectivity is similar to Symmetric Connectivity in that it measures a city in terms of its connection to other cities. However, this metric gives larger weighting to cities with larger local presence, thus giving asymmetric weights that favor cities with more headquarters and less small firm branches. This is calculated in Equation 17.

$$C_i^{Asymmetric} = \sum_f \sum_j \frac{2v_{fi}}{v_{fi} + v_{fj}} \tag{17}$$

Isolated Connectivity separates a city from the World City Network and only analyzes the local presence of all firms in that city, as shown in Equation18.

$$C_i^{Isolated} = \sum_f v_{fi} \tag{18}$$

These three measures of Connectivity do not drastically differ from each other, though they allow for an interesting analysis of the symmetry of these global firm connections. Additionally, we found that these Connectivities demonstrate power-law scaling as in Equation 1 with $\beta < 1$, with β varying between the indicators, as shown in Figure 7.

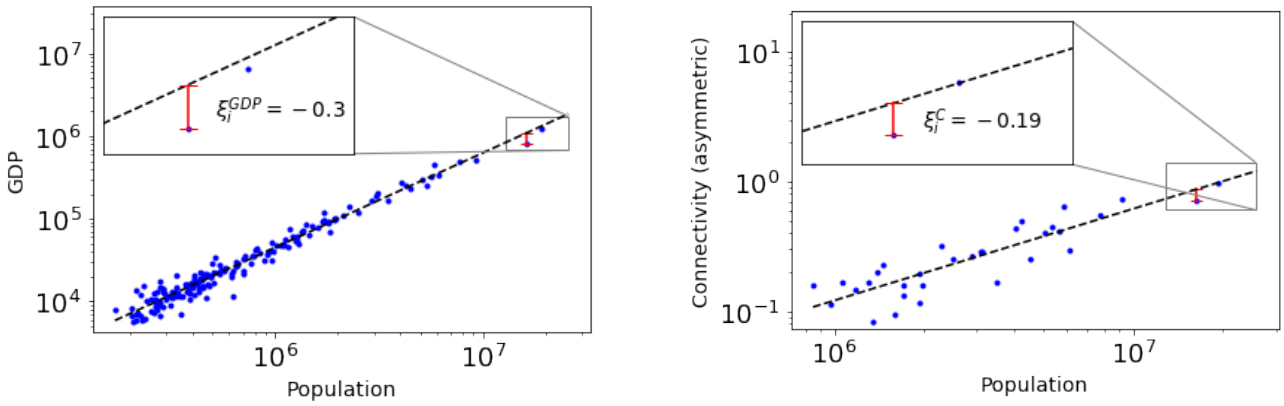

Figure (8) Demonstration of calculating SAMIs ξ_i as explained in section 1.2 and used in the analyses in section 2. Both plots are scaling plots as in Figure 1, the left plot showing GDP scaling, the right plot showing global Connectivity scaling. Every blue dot is a US Metropolitan Statistical Area, with the SAMI for GDP and Connectivity shown in both plots for the Los Angeles Metropolitan Statistical Area, showing that Los Angeles both has a smaller GDP and is less globally connected than expected given its population size.

The core method of analysis here is similar to that used in the study highlighted in Section 1.2 from Bettencourt et al. measuring cross-correlations of Scale-Adjusted Metropolitan Indicators. In this study, we measure cross-correlations between network connectivity measures (air traffic and the three forms of global firm connectivity) and three urban indicators: GDP, patent production, and unemployment. The fitting procedure is done by fitting Equation 1 to aggregated data of all cities in the dataset, primarily US Cities and European cities from UK, Spain, Germany, France, and Italy. The fitting is done using a least-squared-error method with residuals calculated in log-log space. The deviations from scaling prediction are measured using Scale-Adjusted Metropolitan Indicators (SAMI) from Bettencourt et al. [8], defined in Equation 3.

	Global Firm Connectivity (Symmetric)	Global Firm Connectivity (Asymmetric)	Isolated Firm Connectivity	Air Traffic
GDP	$R = 0.55$ $^{**}p = 6.9 \times 10^{-8}$	$R = 0.55$ $^{**}p = 3.1 \times 10^{-8}$	$R = 0.60$ $^{**}p = 1.4 \times 10^{-9}$	$R = 0.17$ $p = 8.9 \times 10^{-2}$
Patents	$R = 0.46$ $^{**}p = 1.5 \times 10^{-3}$	$R = 0.48$ $^{**}p = 9.2 \times 10^{-4}$	$R = 0.51$ $^{**}p = 4.6 \times 10^{-4}$	$R = 0.10$ $p = 3.5 \times 10^{-1}$
Unemployment	$R = -0.48$ $^{**}p = 1.1 \times 10^{-3}$	$R = -0.51$ $^{**}p = 4.7 \times 10^{-4}$	$R = -0.53$ $^{**}p = 2.4 \times 10^{-4}$	$R = -0.15$ $p = 2.6 \times 10^{-1}$
	*Notes: *p<0.05, **p<0.01*			

Table (2) Pearson correlation coefficients (R) and p-values (p) for regressions of scaling deviations shown in Figure 9

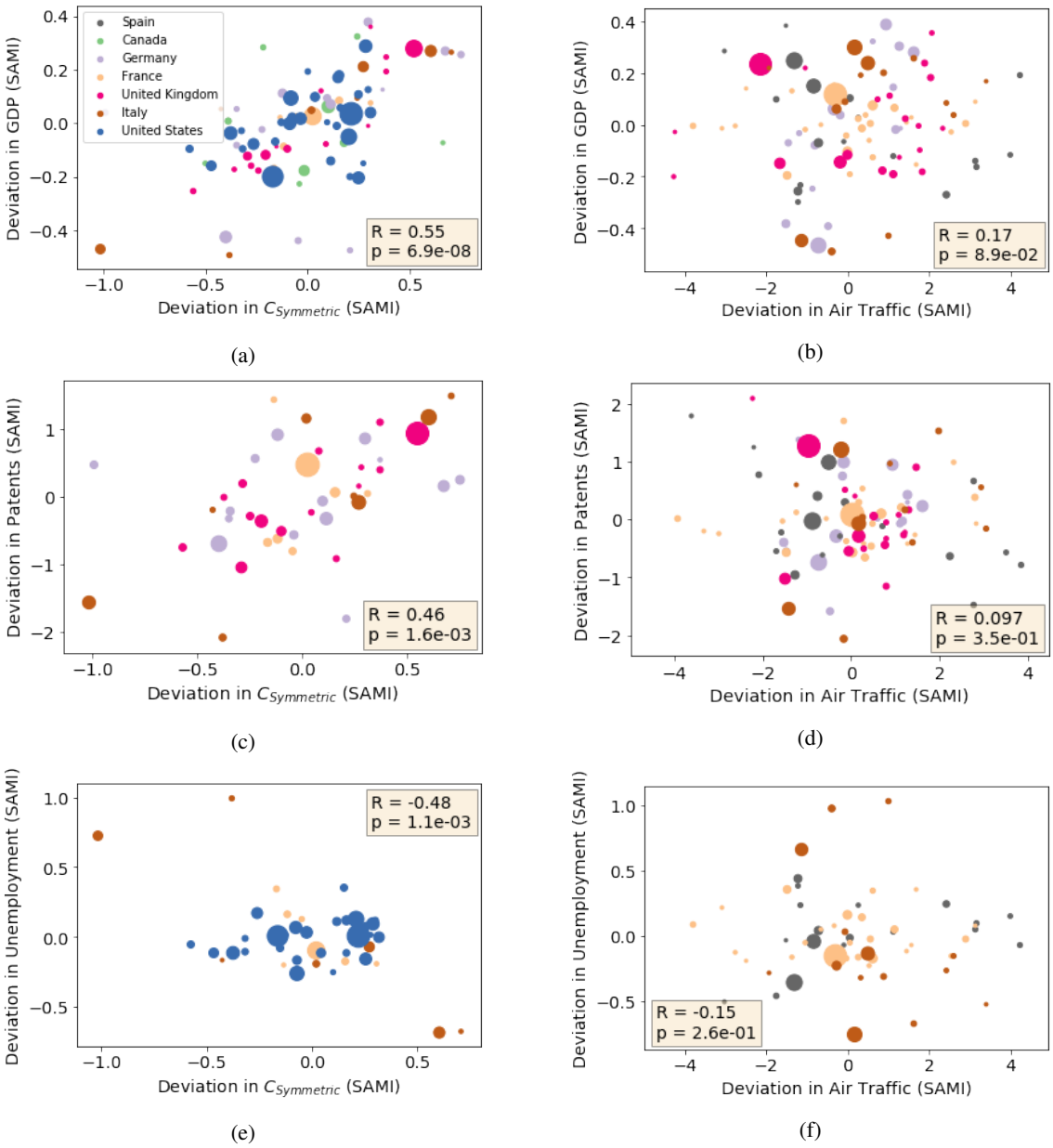

Figure (9) SAMI Deviations in GDP, patent production, and unemployment, compared to SAMI deviations in two measure of inter-urban network connectivity: global firm presence (symmetric, as in Equation 16) and air traffic. Size of points indicates population of city, demonstrating the scale-invariance of the observed trends.

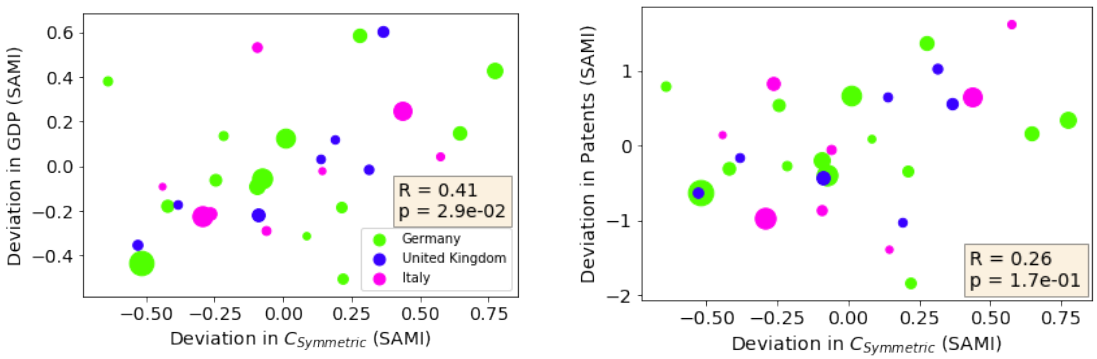

(a) (b)

Figure (10) SAMI Deviations in GDP and patent production plotted against global firm presence (symmetric) using total employed persons as population measure. For GDP vs. firm presence, $R = 0.41$,$p = 2.9\times10^{-2}$. For patents vs. firm presence, $R = 0.26$,$p = 1.7\times10^{-1}$.

2.1.2 Results

As shown in Figure 9 and Table 2, there is significant correlation between deviations from scaling predictions for the three urban indicators (GDP, patent production, and unemployment) and deviations from scaling predictions for inter-urban network connectivity. These correlations were much stronger for global firm connectivity metrics than for air traffic. Showing this correlation answers the primary question of this initial investigation, indicating that deviations from scaling predictions may be in part attributable to effects from inter-urban network interactions. This suggests that inter-urban connectivity may be important in understanding why cities deviate significantly from scaling predictions beyond purely local effects; more than effects of the uniqueness of individual cities, these deviations could be due to the effect of strong (or weak) inter-urban network links.

These correlations also show an unexpected asymmetry of city connectivities. The correlations are observed to be stronger for the asymmetric connectivity measure than for the symmetric connectivity measure. Even more surprisingly, the Isolated Connectivity shows by far the strongest correlation. This suggests that firm connections between cities are not necessarily symmetric in their benefits.

It is also observed that the correlations using Air Traffic as a metric for connectivity are much less significant than other measures of connectivity, suggesting that simply the flow of people alone is not what contributes to meaningful city connections, or that while some cross-city social connectivity will contribute meaningfully to a city's performance, most will not. Later, in section 2.2, we use this observation to weight cross-city social connectivity in proportion to their inferred socioeconomic significance.

Lastly, the analysis is repeated, replacing total resident population with the number of employed persons in each city. This is done to consider whether the correlations involving firm presence in Figure 9 are a result of increased local economic activity in a given city. Results shown in Figure 10 show that this does not alter the observed trends or greatly reduce their statistical significance.

While similar studies have explored similar questions in the past [18, 19] regarding the effects of semi-local or non-local interactions in cities, they have done so without taking into consideration perspectives from urban scaling theory. Therefore, the results shown here serve to both reinforce their findings and extend them to the urban scaling literature by suggesting that deviations from scaling are not pure random statistics but can be attributed in part to the effects of inter-urban network interactions.

2.2 Borrowed Size Modeling With Semi-Local Population Estimates

Here, the second primary research question of this section is investigated: Can a new model be proposed to characterize the effects of inter-urban network interactions on scaling properties? In effect, the goal is to produce a model of urban interactions both local and semi-local which can incorporate the effects of inter-urban network interactions on scaling properties uncovered in the previous section. One such model is presented below.

2.2.1 Two Theories of Urban Scaling With Borrowed Size

The borrowed size theory of Alonso, Burger et al. [19, 20], as is reviewed in Section 1.3.2, is formalized here into a modified version of Equation 1, the scaling theory of Bettencourt et al. [7]. Because Equation 1 has such a simple direct dependence on the population, it is easy to propose a borrowed size model that replaces local population with population potential:

$$Y = Y_0 N_{PP}^{\beta} \tag{19}$$

where N_{PP} is the population potential. This population potential can be written as a sum of local population N_L plus an effective non-local population N_{NL}, which comprises the effective number of non-residents who should be incorporated into the city's network of interactions. To attempt to measure N_{NL}, we use the number of Air Traffic passengers entering the city per year, N_V, and scale it by a fit parameter α as seen below in Equation 20 which defines a population potential measurement. Thus, α can be interpreted as a factor describing how many visitors are equivalent to one resident in the population potential.

$$N_{PP} = N_L + \frac{N_V}{\alpha} \tag{20}$$

Combining equations 19 and 20 gives the first of two Borrowed Size models:

$$Y = Y_0 (N_L + \frac{N_V}{\alpha})^{\beta} \tag{21}$$

Next, a Weighted Borrowed Size Model is proposed. Results from section 2.1 suggest that economic inter-urban network interactions are more significant to urban outputs than social inter-urban network interactions, as measured in the data used. Thus, this suggests that certain visiting populations may be more significant to the networks and outputs of a city than others. In other words, a city which is strongly connected to global economic networks will most likely have a higher proportion of visitors who visit to establish productive economic initiatives between different cities which over time produce significant socioeconomic

outputs. To capture this using the data gathered on global firm connectivity, the Weighted Borrowed Size Model is proposed:

$$Y = Y_0(N_L + \frac{C_{actual}}{C_{fit}}\frac{N_V}{\alpha})^{\beta} \tag{22}$$

In Equation 22, C_{actual} and C_{fit} are the actual and predicted global firm connectivities of a given city, respectively, where C_{fit} is derived from fitting Equation 1 to connectivity vs. population, as in Figure 7. The ratio $\frac{C_{actual}}{C_{fit}}$ is equivalent to the SAMI of C without taking the logarithm. For measuring C in Equation 22 in the following section, $C^{Symmetric}$ (Equation 16) is used. This was an arbitrary choice as other metrics of connectivity (such as equations 18 or 17) could be used as well.

The two models, Equations 21 and 22, are equivalent up to the weighting factor $\frac{C_{actual}}{C_{fit}}$ in Equation 22. Therefore, Equation 21 is referred to as the Unweighted Borrowed Size Model and Equation 22 is referred to as the Weighted Borrowed Size Model.

2.2.2 Model Comparisons

Both borrowed size models are compared to the standard Scaling model described by Equation 1. Each model is fit to the scaling distributions for each of the three indicators used above (GDP, patents, unemployment) using least-squared-error method with residuals measured in log-space. Both borrowed size models are compared to standard Equation 1 using Akaike and Bayesian Information Criterion (AIC and BIC) to describe the statistical significance of the accuracy of their fits to the data. This measure accounts for the number of free parameters in a model to provide a goodness-of-fit measure and therefore accounts for the added parameters in the borrowed size model. Treating Equation 1 as the null hypothesis against which equations 21 and 22 are both tested, the differences of AIC and BIC values between the test model and null hypothesis model (H_0) is used as a measure of support for the test model against the standard urban scaling model. Table 3 describes the significance of BIC values, which are similar to that of AIC values. The results are summarized in Tables 4 and 5. These model comparisons are also visualized in Figures 11 and 12. Because of the limited availability of data across the multiple datasets used, only results using GDP are shown here.

Table (3) BIC Model Comparison Significance

Δ BIC	Evidence Against H_0
$1 - 3.2$	Not worth mention
$3.2 - 10$	Substantial
$10 - 100$	Strong
> 100	Decisive

This table was adapted from [45] and characterizes the statistical significance of BIC (and similarly AIC) values in the model comparison results in this section.

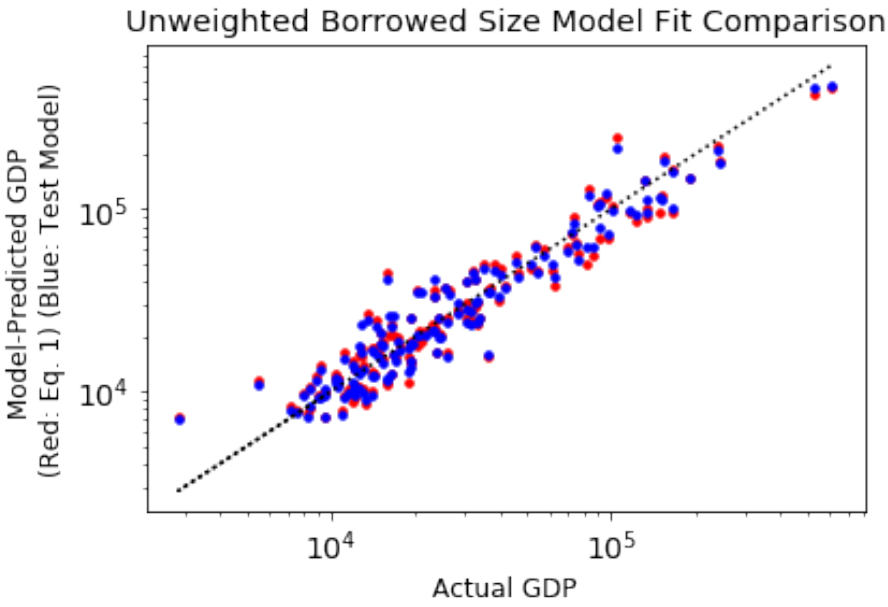

Figure (11) Model Comparison of Standard Scaling (Equation 1) in red to Unweighted Borrowed Size Model (Equation 21) in blue for GDP for 144 European cities across countries. This shows how close each model is to the actual data; the closer a model is to the black dotted line (perfect fit), the more accurate it is.

Table (4) Unweighted Borrowed Size Model Results

Country (n=sample size)	Model Fit Parameters			Model Comparison Measures	
	β (Model: Eq. 1)	β (Model: Eq. 21)	α (Model: Eq. 21)	Δ BIC	Δ AIC
Germany (n=17)	1.15	1.09	5.0	7.2	8.03
Spain (n=19)	1.03	1.03	-340	-2.89	-1.95
France (n=27)	1.12	1.10	20	-1.2	0.1
United Kingdom (n=21)	1.09	1.00	6.0	-0.38	0.67
Italy (n=15)	1.02	1.04	9.0	-0.46	0.24
All European Cities (n=144)	1.07	1.04	13	7.46	10.42

Results for comparing the Unweighted Borrowed Size Model (Equation 21) to the standard urban scaling model (Equation 1). Fit Parameters are shown as well as the Information Criterion model comparison metrics. The BIC and AIC significance is described in Table 3 (with AIC having a similar weighting to BIC).

The statistical significance of all fits are summarized by their Bayesian Information Criterion (BIC) values in Table 4. This measure accounts for the number of free parameters in a model and therefore accounts for the added parameters in the Borrowed Size model.

As demonstrated, this model is a best fit for Germany as well as the agglomeration of numerous European cities across countries. This is also seen qualitatively in fig.11. For Spain, France, UK, and Italy, the Borrowed Size model was about just as good or slightly worse than the model described by Equation 1.

The fit values for the parameter α are also interesting. All countries showed consistency in their α values: They are positive, indicating increasing GDP for cities with more than

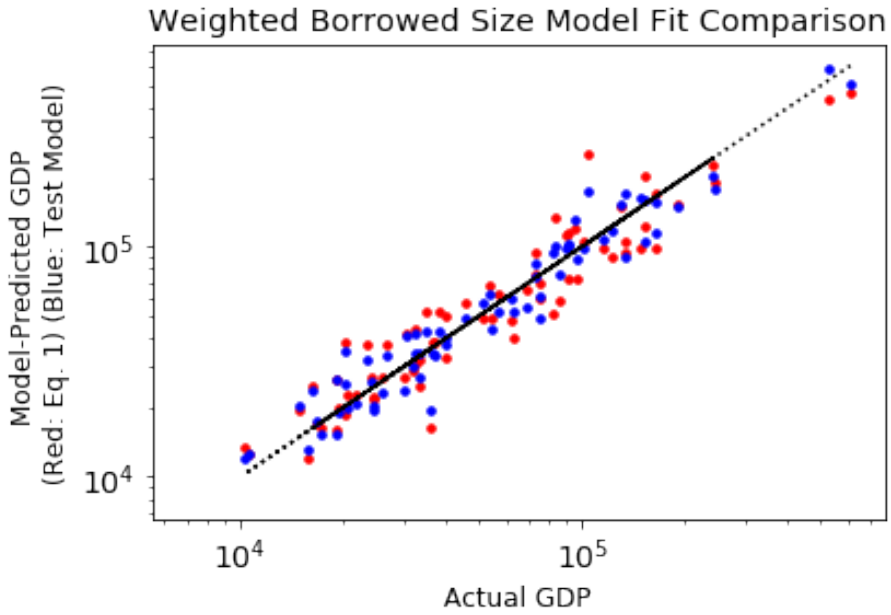

Figure (12) Model comparison of standard urban scaling (Equation 1) in red to Weighted Borrowed Size Model (Equation 22) in blue for GDP for 71 European cities across countries. This shows how close each model is to the actual data; the closer a model is to the black dotted line (perfect fit), the more accurate it is.

average visitors; and they are approximately of the same order. The only outlier was Spain, which demonstrated opposite values for α, indicating a negative effect of visitor population. However, the model did not seem to fit Spain well according to the BIC value.

Table (5) Weighted Borrowed Size Model Results

Country (n=sample size)	Model Fit Parameters			Model Comparison Measures	
	β (Model: Eq. 1)	β (Model: Eq. 22)	α (Model: Eq. 22)	Δ BIC	Δ AIC
Germany (n=11)	1.15	1.10	7.0	5.35	5.76
United Kingdom (n=14)	1.08	0.93	6.0	2.73	3.37
All European Cities (n=71)	1.05	0.95	5.0	33.6	35.86

Results for comparing the Weighted Borrowed Size Model (Equation 22) to the standard urban scaling model (Equation 1). Fit Parameters are shown as well as the Information Criterion model comparison metrics. The BIC and AIC significance is described in Table 3 (with AIC having a similar weighting to BIC).

The same analysis was conducted for the model presented in Equation 22. Though much less data was available which contained both air traffic and global firm connectivity, results were mostly consistent with the model in Equation 21 while showing more significant fits, shown in Table 5 and Figure 12. The most significant model improvement is again in the agglomeration of cities across countries.

2.3 Network Production Model

Section 2.2 proposed a model for the effects of inter-urban network interactions as motivated by previous sociological theories of inter-urban interactions. Here, we formulate a new model for urban outputs which more directly incorporates forms of inter-urban network interactions. In doing so, we rely on a central hypothesis of urban scaling alluded to before: urban outputs are the net result of social interactions [7]. This idea and its implications for scaling theory were discussed in Section 1. While scaling theory considers only local social interactions in this hypothesis, the theory developed in this section expands this hypothesis to also incorporate social interactions that are semi-local in nature. The contribution from semi-local interactions is hypothesized below based on conjectures about the types of social networks generating these interactions.

2.3.1 Theory

The socioeconomic contribution from semi-local interactions is difficult to reliably predict, especially when ill-defined. Here, we postulate that such semi-local interactions may be represented as either Visiting-type interactions or Institutional-type interactions, which add to local interactions to produce a full (local and semi-local) network production model of the form:

$$Y = Y_{Local} + Y_{Visiting} + Y_{Institutional} \tag{23}$$

with $Y_{Local} = Y_{0,L}N_L^{\beta}$ from Equation 1 with N_L representing the local resident population. This term can be understood within the network production model as the net output from N_L^{β} number of social interactions in a city each producing output $Y_{0,L}$. Visiting interactions are understood to be interactions which occur when people travel to a different city. Tourism is the best example of this form of interaction, though individuals visiting a city for business purposes will also interact through these means. Institutional interactions are interactions which are mediated through institutions (e.g. universities, global firms) shared between cities.

First, Visiting interactions are postulated. To start, the urban outputs from visiting interactions can be generally formulated, for N_V visiting population, in the following equation:

$$Y_{Visiting} = Y_{0,V}N_V I \tag{24}$$

in which $Y_{0,V}$ is the average output per social interaction, N_V is the number of visitors, and I is the rate of interaction per visitor

Urban scaling theory emphasizes the spatial nature of local social interactions that produce urban outputs [7]. Because the city environment is effectively the same for a local and for a visitor, a visitor should therefore interact within the city at the same rate as a local. Thus, we derive the per-person interaction rate from Equation 1:

$$Y_{Local} = Y_{0,L}N_L^{\beta} = Y_{0,L}N_L^{1+\delta} = Y_{0,L}N_L^1 N_L^{\delta} = Y_{0,L}N_L I \tag{25}$$

$$\implies I = N_L^{\delta} \tag{26}$$

where $\beta = 1 + \delta$. Thus, the average number of interactions any one person will have while in a city is $I = N_L^{\delta}$. Because this interaction rate is hypothesized to be approximately the

same for local and visiting populations (though perhaps with a smaller interaction output $Y_{0,V}$), this rate is also applied to interaction rates of visitors. Thus, substituting $I = N_L^\delta$ into Equation 24 suggests

$$Y_{Visiting} = Y_{0,V} N_V N_L^\delta \tag{27}$$

This is the proposed contribution to urban outputs from Visiting-type interactions produced within an inter-urban network, the second term in Equation 23.

The second proposed term accounting for inter-urban network interactions is an Institutional term, which comprises direct links between institutions in cities, often dominated by economic interactions and which may or may not also be accompanied by Visiting-type inter-urban interactions. The co-presence of global firms examined in section 2.1 is a clear example of these sorts of ties.

In the largest limiting case, Institutional contributions could be proportional to $N_I N_L$ for N_I the of interacting semi-local institutions (e.g. global firms) and N_L again the local population: For every semi-local institution N_I, there could be N_L connections formed with every resident of the city. However, it is expected that institutional interactions are more isolated in nature than visiting or local interactions, and therefore the output of institutional interactions would not be proportional to N_L. This means that the urban outputs created by semi-local institutional interactions would be proportional only to the number of interacting institutions N_I. With institutional interactions creating an average output Y_1, this implies

$$Y_{Institutional} = Y_{0,V} N_I \tag{28}$$

Thus, a new comprehensive model of urban scaling (Equation 1) which accounts for Visiting-type and Institutional-type inter-urban network interactions is postulated as

$$Y = Y_{0,L}(N_L)^{1+\delta} + Y_{0,I} N_I + Y_{0,V} N_V N_L^\delta \tag{29}$$

This equation above can be easily fit to data a similar way as in Section 2.2. To do so, N_V is fit to $\frac{N_{AT}}{\alpha}$, with α to normalize the number of air traffic passengers that equals one effective visitor, rewriting Equation 30 as

$$Y = Y_{0,L}(N_L)^{1+\delta} + Y_{0,I} N_I + Y_{0,V} \frac{N_V}{\alpha} N_L^\delta \tag{30}$$

Results for this analysis are shown below in Section 2.3.2.

2.3.2 Results

As shown in Table 6, this model is a significant improvement to standard scaling for all countries analyzed, as measured by Bayesian (BIC) and Akraine (AIC) information criteria values which measure two models' strength of fit accounting for the number of fit parameters. This can also be seen in Figure 13, which shows a comparison of the two models. It is also noteworthy that, while the model is still a significant improvement for all countries with sufficient data, this new model is most effective at fitting data from across countries. This aligns well with the fact that cities' integration into inter-urban networks is highly dependent on national-level policy; standard scaling which only accounts for local interactions does not account for these significant differences across nations of inter-urban network integration.

Interestingly, α from Equation 30 is measured as the same value measured when fitting the weighted borrowed size model in Section 2.2, Equation 21. Note that while the α values are differently constructed in the two equations, they are qualitatively measuring the same thing: how many visitors it takes to make an equal contribution to a city's net outputs as one local resident.

This model also gives a very insightful measure of the local vs. semi-local contributions to a city's output, as summarized in Table 7 by calculating the ratios of the values of each term in Equation 30. According to this model, using the agglomerate data of all countries in the dataset, this suggests that 69% of socioeconomic outputs in a city are produced by local interactions, while inter-urban network interactions account for the other 31% (13% Visiting and 18% Institutional).

Table (6) Urban Network Production Model Results

	Model Fit Parameters			Model Comparison Measures	
Country (n=sample size)	β (Model: Eq. 1)	β (Model: Eq. 30)	α (Model: Eq. 30)	Δ BIC	Δ AIC
Germany (n=11)	1.15	1.15	4	3.7	4.5
United Kingdom (n=14)	1.08	1.35	60	13.5	14.8
All European Cities (n=71)	1.05	1.08	4	40.4	44.2

Results for comparing the Urban Network Production Model (Equation 30) to the standard urban scaling model (Equation 1). Fit Parameters are shown as well as the Information Criterion model comparison metrics. The BIC and AIC significance is described in Table 3 (with AIC having a similar weighting to BIC).

Table (7) Local, Visiting, and Institutional contributions

Country	Average **Local** Term (Proportion of Total)	Average **Visiting** Term (Proportion of Total)	Average **Institutional** Term (Proportion of Total)
Germany	0.74	0.23	0.03
United Kingdom	0.62	-0.03	0.41
All Countries	0.69	0.13	0.18

Average contributions to Y (GDP) from each term in Equation 30 (corresponding to Equation 23). Calculated using the agglomerate of all European cities with data (last row in Table 6).

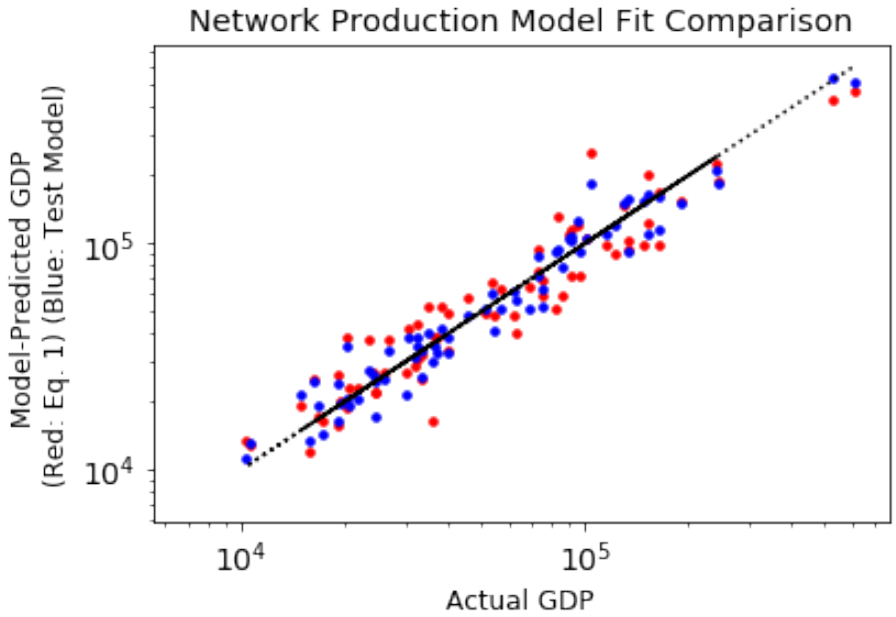

Figure (13) Model Comparison of Standard Scaling (Equation 1) in red to the Urban Network Production Model (Equation 30) in blue for GDP for 71 European cities across countries. This shows how close each model is to the actual data; the closer a model is to the black dotted line (perfect fit), the more accurate it is.

2.4 Conclusion & Discussion

Through empirical analyses of inter-city network interactions using different measurements of inter-city networks, this research has demonstrated a significant effect of inter-city network connectivity on some urban functions beyond that explained by urban scaling alone. By formalizing and empirically testing different models that incorporate inter-city interactions into an urban scaling framework, this work provides an additional perspective to the existing theoretical model of urban scaling. This added perspective suggests that while socioeconomic outputs in a city are dominated by local interactions, non-local interactions (inter-urban network interactions) also are an important contributing factor. Precisely, the final model tested suggests that about 70% of superlinear scaling outputs are attributable to local size effects while 30% are attributable to inter-city network effects. The same ratio of local vs. global significance was found by Meijers et al. in a similar study [18].

There are two important caveats to these results. First, most of the metrics used for this analysis are economic, thus one cannot conclude that these effects extend to other examples of superlinear urban scaling such as crime rates and patent production. Second, this analysis does not demonstrate causality. The cross-correlation of Scale-Adjusted Metropolitan Indicators for inter-city network connectivity and various urban indicators such as GDP shows only correlations. It is possible that connectivity promotes urban outputs or vice-versa, or that a separate effect drives both simultaneously. Thus, these results are just a first attempt to extend urban scaling theory to the inter-city level and empirically test the resulting hypotheses.

Future work should be done to verify these results across regions, time periods, and metropolitan indicators. It would be especially insightful to measure the local vs. non-local contributions reported in Table 7 for other metrics to understand the locality of these metrics. For instance, one would expect that crime is a nearly 100% local output whereas patents may be below 50% local. Developing more rigorous models for inter-city networks within the urban scaling framework would also lay the groundwork for future work connecting urban scaling research with global and world city research.

This works provides a new and valuable insight into aspects of modern cities which the urban scaling literature may currently overlook, particularly the potentially growing effect of inter-city networks. While this work uses ideas and methods from global and world city literature to extend Urban Scaling Theory to the inter-city level, it also connects disciplines the other way: The tools and ideas from urban scaling theory offer new and valuable insights into how the global urban system affects metropolitan functions in a city. Therefore, this work serves as a bridge between the urban scaling literature and the global and world city literature. Understanding the relationship between urban scaling and inter-city networks is important for two reasons. This may provide a more complete theoretical understanding of urban dynamics, contributing to research in urban science. Additionally, inter-city network effects have important implications for policies which directly and indirectly mediate these inter-city networks and their impacts on the people living within cities.

3 Connecting Intra-urban Network Structure with Urban Income Inequality

Section 1.4 discusses existing research on two topics within Urban Science: Intra-urban interaction networks and urban income inequality. Most of the existing research on these two important topics does not intersect, however Section 1.4 demonstrated that there is some evidence to show that the structure of the intra-urban network is important to understanding the nature of urban income inequality and other examples of distributional effects of scaling properties within cities. The central hypothesis of the original work in this chapter is that there is a significant relationship between intra-urban network structures and distributional effects within cities. This hypothesis is tested using Kinetic Exchange Modeling of interactions within a wide variety of intra-urban network structures in comparison with a detailed empirical analysis of income distributions in US Metropolitan Areas.

3.1 Empirical Analysis of Income Distributions Across US Cities

We begin by reproducing a similar empirical result to Figure 4 from Sarkar et al. [24] in showing urban allometry in income distributions. An analysis originally conducted by Cate Heine [46] and recreated here demonstrates a different scaling behavior for different segments of urban populations. The population of each city is separated into deciles based on income and the scaling of each decile across city size is measured. If different populations within a city were to scale homogeneously across city size, then it would be expected that the scaling behavior of each decile would be characterized by Equation 1 with higher/lower Y_0 and fixed scaling exponent β. Instead, it is shown that lower income deciles scale sub-linearly ($\beta < 1$) while the highest income deciles scale very super-linearly ($\beta > 1$). A more detailed analysis of income distributions across city size provides a clearer picture of the nature of these income decile scaling effects.

The primary dataset used in this study is from the 2015 American Community Survey conducted by the US Census Bureau. Incomes are reported for every metropolitan and micropolitan area in the US and are aggregated by census tracts, small local areas of on average 4500 people, of which on average 2300 report income. Figure 14 demonstrates the distribution of the number of census tracts per city.

To interpolate and extrapolate from this aggregated distribution to an approximation of a individual-level distribution, we use a Gaussian Kernel Density Estimator with a widened Silverman bandwidth function. Effectively this extrapolates the average reported income of each census tract (each small blue line in Figure 15) to a Gaussian Probability Distribution Function (PDF) with a mean equal to the reported income average, and the standard deviation calculated as a function of the number of datapoints. Summing the Guassian PDFs for each census tract produces a full PDF for a city, seen in the red curves in Figure 15. This method assumes that individuals within each census tract have incomes distributed normally around the reported mean income of that census tract. This produces estimated PDFs of income at the individual level for each Metropolitan Statistical Area (MSA) and Micropolitan Statistical Area (MiSA) in the United States. Examples of four cities ranging from the smallest to largest metropolitan areas are shown in Figure 15.

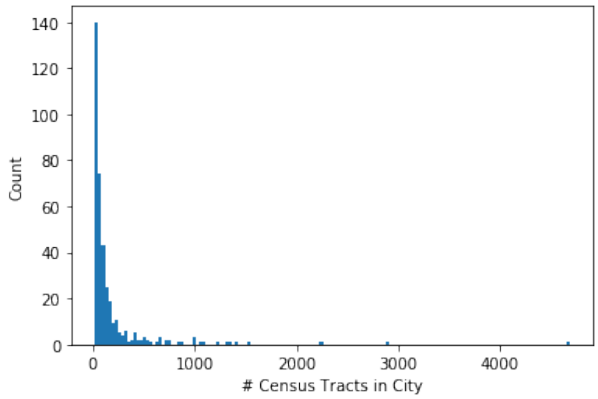

Figure (14) Histogram of number of census tracts for in different US MSAs.

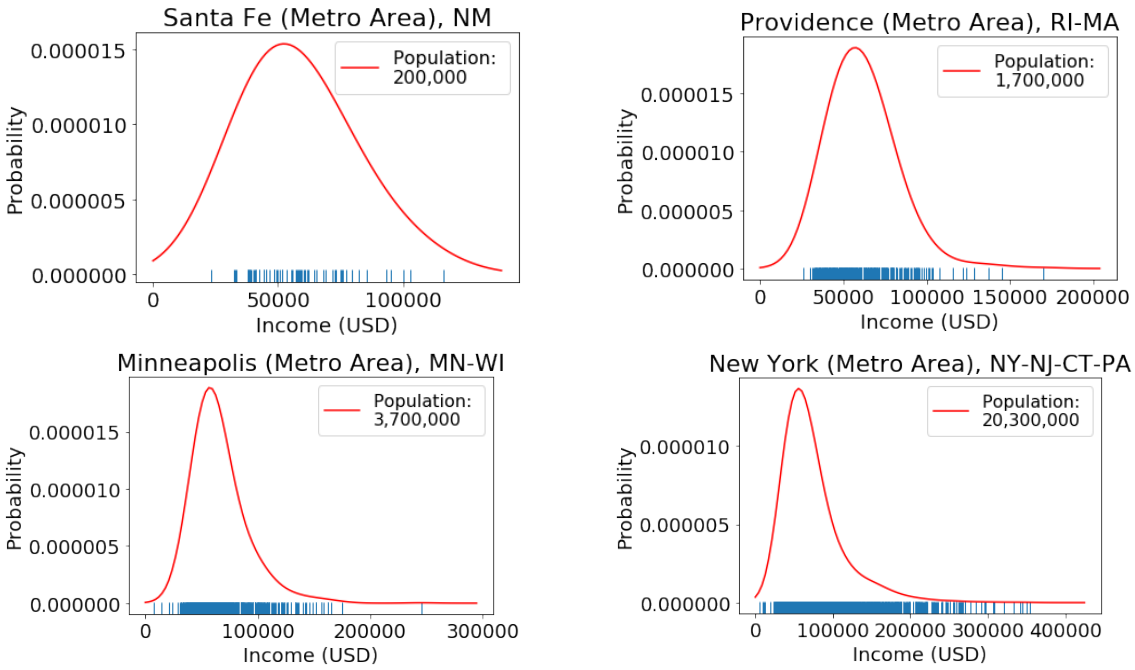

Figure (15) Estimations of individual income distributions using Gaussian Kernel Density Estimation (KDE) on census tract data. Each figure is a rugplot in which the blue marks represent each reported census tract, and the red curve is the pdf generated from a Gaussian KDE.

The estimated income distributions for US cities, as found above, are separated into deciles: 10% of the population which reports the lowest income is grouped into the first decile (decile #1), and likewise for all ten deciles up to the 10% of the population which has the highest income (decile #10). The scaling behavior of each decile across city size is then analyzed by fitting Equation 1 to the summed or average decile income vs. population across all MSAs, once for each decile. These results are plotted in Figure 16.

For lower deciles, β is mostly linear or slighly sublinear, as low as 0.97. For upper deciles, β is consistently superlinear, as high as 1.16. These results are similar to the Australian study which found $\beta \in [0.94, 1.00]$ for lower income groups and $\beta \in [1.00, 1.21]$ for higher income groups [24], as shown in Figure 4. This shows that different populations within cities scale differently, and that scaling effects are not equivalent for all segments of the population; in fact, the poorest populations are observed to be even poorer in bigger cities. This again aligns with existing research showing that larger cities are more unequal [28, 26, 27]. It is also important to note the slight methodological difference between the analysis conducted here (Figure 16) and that from Sarkar et al. [24, 25] in Figure 4. While Sarkar's study sorts every city into subgroups defined by consistent income brackets (e.g. \$20,000-\$40,000), this study sorts cities into ten subgroups by percentiles of income within each city. Thus, decile 1 in city A may range from income \$0 to \$20,000 while decile 1 in city B may range from \$0 to \$25,000.

Next, we wanted to more precisely characterize how income distributions change across city size in order to better empirically understand the phenomenon of subgroup scaling differences captured in Figure 16. The observed scaling behavior of different deciles is itself a meaningful characteristic of how income distributions scale by size, but do not present the full picture of how populations might benefit more or less from urban agglomeration effects. To better characterize these incomes distributions, we analyzed how their statistical moments change with city size. We chose to examine the first four moments: Mean, variance, skewness, and kurtosis.

In Figure 17, it is seen that there are significant trends in the statistical moments of the income distributions. The first moment, the mean, shows the well-characterized urban agglomeration effect: per capita outputs (income in this case) increase with city size [1]. Interestingly, the second, and third moments both increase similarly with city size, suggesting a widening of the distribution and a growing tail. This can also be qualitatively observed in the example distributions in Figure 15. Lastly, the kurtosis (4th moment) also increases with population size, showing an increase in the "tailedness" of the distribution.

Together, these empirical characteristics of income distributions across US cities are significant results in their own right, demonstrating alternative scaling behavior of subgroups in cities rarely observed before. We believe these distributional characteristics of urban agglomeration effects are important and deserve more study. The results in this subsection also serve as an empirical benchmark for the Kinetic Exchange Modeling that encapsulates the bulk of this chapter, as is discussed in the following section.

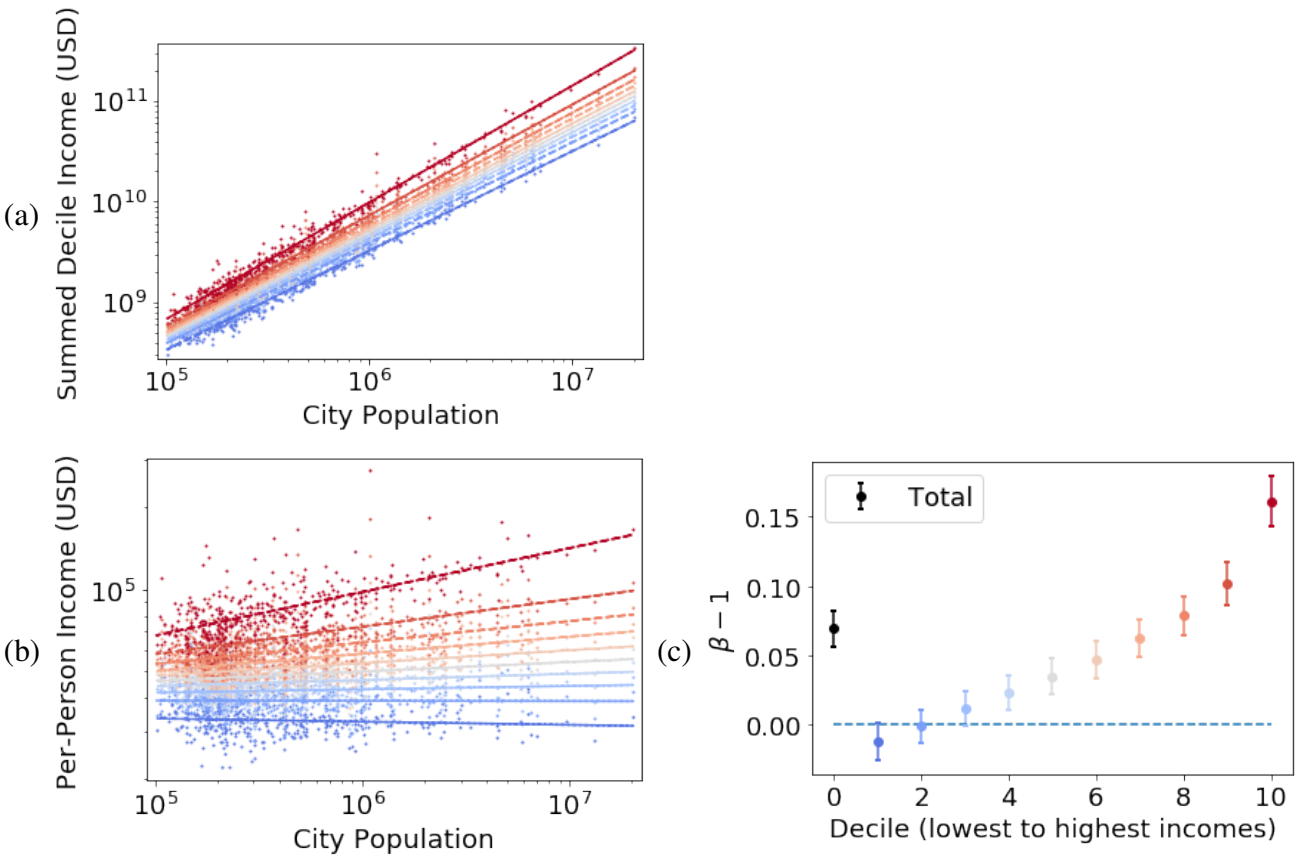

Figure (16) Scaling of income across population size for income-based deciles of US MSAs. Across all figures, the darkest red represents the highest-income decile while the darkest blue represents the lowest-income decile. (a) Scaling of total income (b) Scaling of per-person income (c) 95% Confidence Intervals for Scaling exponents of each decile as well as Total scaling exponent, demonstrating higher-income deciles scaling more superlinearly than lower and middle-income deciles.

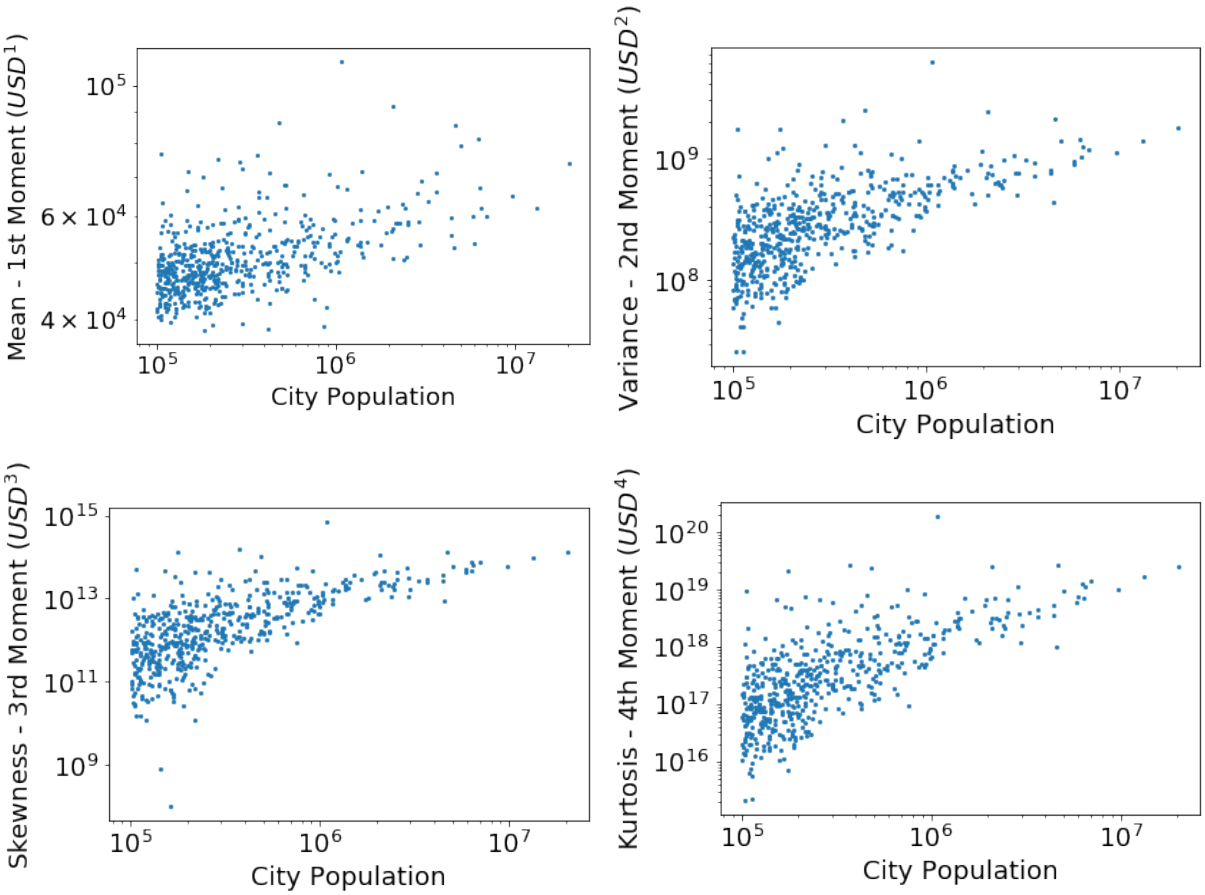

Figure (17) Statistical moments (1-4) vs. population for all US MSAs

3.2 Kinetic Exchange Modeling of Income and Wealth

The empirical characteristics of income distributions in the US are a phenomenon of urban scaling not yet well-understood. When Sarkar et al. first observed them, they noted "The full set of social and economic processes that could explain our observations are complex, interconnected and varied, and need to be examined in detail in future work. Only then will it be possible to provide some specific policy advice about how we can grow our cities in ways which reduce the levels of inequality" [24]. In effect, the work of this section is an attempt to uncover these social and economic processes at work in producing the empirical characteristics uncovered in Section 3.1 via Kinetic Exchange Modeling, a method reviewed in Section 1.5. The choice of using Kinetic Exchange Models (KEMs) is founded on a central hypothesis from urban scaling theory referenced throughout this paper: Urban outputs are aggregate outputs of social interactions [7]. This section attempts to use Kinetic Exchange Models to build an agent-based model for these social interactions. This allows for an analysis at the microscopic level of the forms of social networks in cities which could demonstrate the phenomena uncovered in Section 3.1. Specifically, we attempt to model types of social network structures and interaction mechanisms which could produce the following distinguishing distributional characteristics:

1. Decile scaling differences as shown in Figure 16. This specifically refers to the approximately linear positive relationship between income decile and decile scaling exponent β characterized in Figure 16, subfigure (c).
2. Shape of income distributions characteristically similar to the income distributions shown in Figure 15. While the general shape of the distribution is certainly of interest, for the purposes of this study (as it relates to the urban scaling literature), the relationship with city-size characterized in Figure 17 is more significant.
3. General superlinear scaling of combined income.

To achieve the modeling objectives listed above, the key analysis of these Kinetic Exchange Models (KEM) must be their size-variance. How do the distributions each KEM produces change over the size of the population of agents in the model? Thus, we simulate multiple KEMs with agent populations varying from approximately 300 to 5000. These distributions allow for cross-comparison to the analyses done in Section 3.1.

3.2.1 Kinetic Exchange Modeling on Non-Trivial Network Structures

In attempting to construct KEMs which best model the types of intra-urban interaction networks explored in Section 1.3, we chose to incorporate non-trivial network structures into Kinetic Exchange Modeling. The overwhelming majority of existing research using KEMs models interactions on simple networks like a random or fully-connected network [38]. Some researchers have begun to explore KEMs modelled on non-trivial network topologies, either in fully-connected but directed networks or in rewiring networks with preferential attachment [47]. Still, most of these studies appear not to explore KEMs operating on many other network structures, particularly networks topologies associated with real-world social networks, such as small-world or scale-free networks [48, 49].

For this study, we analyze KEMs simulated on 3 network structures: small-world, scale-free, and random. A random network is the simplest, consisting of randomly adding interaction edges between every pair of agent nodes with a fixed probability. The small-world network is constructed by initially connecting each node with its k nearest neighbors, and with small fixed probability p removing a local edge and replacing it with an edge to a random distant node [48]. The small-world network derives its name from the popular notion of "6 degrees of separation," derived from a study showing that two randomly selected people geographically separated were, on average, only 6 degrees of separation from each other [50]. In the language of network science, this means the average path length between nodes in a small-world network is small. This is achieved by the random rewiring to long-distance edges. Another real-world phenomenon modeled by the small-world network is "tight-knit" communities: Most of an individual's neighbors are also connected with each other. In network science, this translates to a high clustering coefficient, defined as the average probability that two of one nodes' neighbors are neighbors to each other [48].

A scale-free network is most distinctly characterized by a power-law degree distribution. This means that the probability a node has k number of neighbors can be modeled by

$$P(k) = k^{-\gamma}$$

usually with $2 < \gamma < 3$ [49]. This is quite often observed in real-world social networks [49]. One method to construct a scale-free network is the Barbasi-Albert method, used here. This method utilizes preferential attachment, which itself has sociological and empirical motivation [49]. Nodes are added to the network one at a time, and every time a node is added, it establishes an edge with an already-existing node with a probability proportional to the number of edges the existing node has. Thus, early nodes quickly develop large numbers of edges which makes later nodes preferentially attach to these early nodes even more. This produces a robust scale-free network.

With these three network structures established, we test one more component of these networks: edge density. As motivated by the observation of real-world urban interaction networks densifying over city size (seen in Figure 3), we also test two versions of each of these network structures: A static version and a densifying version. The static version maintains the same average nodal degree $< k >$ over population size. The densifying version replicates the observation in [3] that

$$< k > \propto N^{\beta-1}$$

We use $\beta = 1.2$ as in the empirical study [3] and choose the proportionality factor according to a fixed maximum average degree (set to 50). All together, this produces six network structures on which our KEMs are simulated:

- Random (Static) Network
- Random (Densifying) Network
- Small-world (Static) Network
- Small-world (Densifying) Network
- Scale-free (Static) Network

- Scale-free (Densifying) Network

3.2.2 Simultaneous Interaction and Modified KEMs

In order to both optimize the efficiency of the simulation and better reflect the real-world dynamics of social interactions taking place in real time, interactions in the Kinetic Exchange Models are simulated simultaneously over every edge in the network. This is a slight modification to most KEMs which simulate one edge interaction per timestep. This requires a reformulation of the KEM interaction mechanisms described in Section 1.5. First, we describe the reformulation of the specific KEM mechanism described in section 1.5.1, referred to from now on as the IPDO, short for the Inequality Process with Distributed Omega, as it was titled in its original formulation [42]. The IPDO in its original form can be described by the update function for agents i and j's wealth w from timestep t to $t+1$:

$$w_j(t+1) = \lambda_j w_j(t) + \epsilon((1-\lambda_j)w_j(t) + (1-\lambda_i)w_i(t)) \tag{31}$$
$$w_i(t+1) = \lambda_i w_i(t) + \overline{\epsilon}((1-\lambda_j)w_j(t) + (1-\lambda_i)w_i(t)) \tag{32}$$

where ϵ is a random number in $[0,1]$, $\overline{\epsilon} = 1-\epsilon$, and λ_i is the savings rate of agent i, chosen randomly from a power-law distribution [42].

To reformulate this update function into one for simultaneous interactions, it must be generalized to a vector equation for updating all wealths $\vec{w}$ with one update function. This vector formula for updating agents' wealth can best be described by first redefining the multiplicative exchange element of the IPDO. In the standard IPDO, each agent saves $\lambda_i w_i$ and exchanges $(1-\lambda_i)w_i$ with the single agent it interacts with. In this network KEM, one agent can have many neighbors to interact with simultaneously, so instead we define $\vec{T}$ as the amount that an agent exchanges with each of their neighbors, such that $(1-\lambda_i)w_i = k_i T_i$ (where k_i is the number of neighbors agent i has):

$$T_i = \frac{(1-\lambda_i)w_i}{\sum_j G_{ij}} \tag{33}$$

where G is the adjacency matrix of the network; $G_{ij} = G_{ji} = 1$ if agents i and j have an edge directly connecting them and $G_{ij} = G_{ji} = 0$ if they do not. Thus, $\sum_i G_{ij}$ is the number of neighbors agent i has (equivalent to k_i). This definition of T is interpreted simply as splitting each agent's total exchange amount equally between each of their neighbors.

Next we define a matrix $\mathcal{E}$ representing the random exchange values ϵ in Equation 32. It is required that $\mathcal{E}_{ij} = 1 - \mathcal{E}_{ji}$, given that $\overline{\epsilon} = 1-\epsilon$ in Equation 32 representing the two agents "splitting the pot" of the sum amount that both agents interact with. Additionally,

$$G_{ij} = 0 \implies \mathcal{E}_{ij} = 0$$

because agents who are not connected should exchange zero wealth. Lastly, $\mathcal{E}_{ii} = 0 \; \forall \; i$ because an agent does not interact with itself. All together, this definition of $\mathcal{E}$ is summarized as:

$$\mathcal{E}_{i,j} = \begin{pmatrix} \mathcal{E}_{1,1} & \mathcal{E}_{1,2} & \cdots & \mathcal{E}_{1,n} \\ \mathcal{E}_{2,1} & \mathcal{E}_{2,2} & \cdots & \mathcal{E}_{2,n} \\ \vdots & \vdots & \ddots & \vdots \\ \mathcal{E}_{n,1} & \mathcal{E}_{n,2} & \cdots & \mathcal{E}_{n,n} \end{pmatrix} \tag{34}$$

where

- $\mathcal{E}_{ij} = 1 - \mathcal{E}_{ji}$
- $\mathcal{E}_{ii} = 0 \; \forall \; i$
- $G_{ij} = 0 \implies \mathcal{E}_{ij} = 0$
- n is the number of agents (nodes)
- $\mathcal{E}_{ij} \in [0, 1]$, generated randomly at every timestep

For example, if there are only two agents in the system and they are connected by a node, then $\mathcal{E}$ could be:

$$\mathcal{E}_{i,j} = \begin{pmatrix} 0 & 0.2 \\ 0.8 & 0 \end{pmatrix}$$

Finally, this allows for a complete definition of the IPDO KEM mechanism in a simultaneous interaction KEM:

$$\vec{w}(t+1) = \vec{\lambda} \circ \vec{w}(t) + \mathcal{E}\vec{T}(t) + (\sum_j \mathcal{E}_{ij}) \circ \vec{T}(t) \tag{35}$$

w and λ are the vectors for wealth and savings rates, respectively, so that agent i has wealth w_i and saving rate λ_i. The operation $\circ$ is the Hadamard product, the element-wise multiplication of two vectors ($\circ : \mathbb{R}^n \times \mathbb{R}^n \mapsto \mathbb{R}^n$) such that $(\vec{\lambda} \circ \vec{w})_i = \lambda_i w_i$. The first term represents the savings of each agent, the second term represents the amount each agent i takes from each agent's T_j and the final term represents the amount agent i keeps from its own T_i.

Next, we develop an extended IPDO with growth from interactions. The motivation is to test a KEM in which agents grow their wealth from having increased interactions, as suggested from studies of network diversity [30] and a key hypothesis of urban scaling theory that outputs are proportional to social interactions [7]. This interaction-based growth is achieved by defining a new exchanged vector $\vec{T}^g$ according to:

$$T_i^g \equiv T_i + r(\sum_j G_{ij})T_i \tag{36}$$

where r is a small growth rate (e.g. $r = 0.03$). The wealth updating function for this KEM is then equivalent to the standard IPDO after replacing $\vec{T}$ with $\vec{T}^g$:

$$\vec{w}(t+1) = \vec{\lambda} \circ \vec{w}(t) + \mathcal{E}\vec{T}^g(t) + (\sum_j \mathcal{E}_{ij}) \circ \vec{T}^g(t) \tag{37}$$

Lastly, we define the third and final KEM analyzed here: Multiplicative Exchange with Wealth Accumulation (MEWA). This KEM is a bit more complex in that every agent has both an income I_i and a wealth w_i at each time step, where $I_i = \frac{dw_i}{dt}$. Thus, the wealth update function is only

$$w_i(t+1) = w_i(t) + I_i(t)$$

which in simulatenous interaction is simply

$$\vec{w}(t+1) = \vec{w}(t) + \vec{I}(t) \tag{38}$$

The income of agents is what undergoes both multiplicative exchange and wealth accumulation according to:

$$I_i(t+1) = rw_i(t) + \sum_j G_{ij} T^I(t) \tag{39}$$

in which T^I is defined similarly as in Equation 40 but instead for income:

$$T_i^I = \frac{(1-\lambda_i)I_i}{\sum_j G_{ij}} \tag{40}$$

The second term in Equation 39 represents non-stochastic multiplicative exchange as in Equation 13.

The three KEMs defined above are summarized:

- **IPDO**: This simulates stochastic multiplicative exchanges of wealth between agents. This KEM has zero growth and thus $\overline{w}(t) = \overline{w}(t=0) \forall t$.
- **Growth IPDO**: This is equivalent to the standard IPDO but incorporates a growth component driven both by an agent's wealth and its number of neighbors (more neighbors produces higher growth)
- **MEWA**: This model simulates similar multiplicative exchange as the IPDO but without the stochastic component. Additionally it incorporates a growth term through wealth accumulation.

3.2.3 Kinetic Exchange Modeling Results

We simulated Kinetic Exchange Models of every pair of network (from the networks listed at the end of Section 3.2.1) and KEM mechanism (from the KEMs listed at the end of Section 3.2.2) on populations varying from population sizes between order 10^3 and 10^4. The specific objectives of this modeling were listed at the beginning of Section 3.2. All of the KEMs selected approximately reproduce average income distribution shapes. The most important characteristic to investigate through these models is the decile scaling results shown in Figure 16. Therefore, in Figures 18, 19, and 20 we reproduce the decile scaling exponent relationship for each model. These are produced exactly the same way as in Figure 16, thus Figure 16 serves as a point of empirical comparison for each of the model results presented. a positive relationship between β and decile n implies higher-income decile groups scale more superlinearly than lower-income decile groups. The only models which

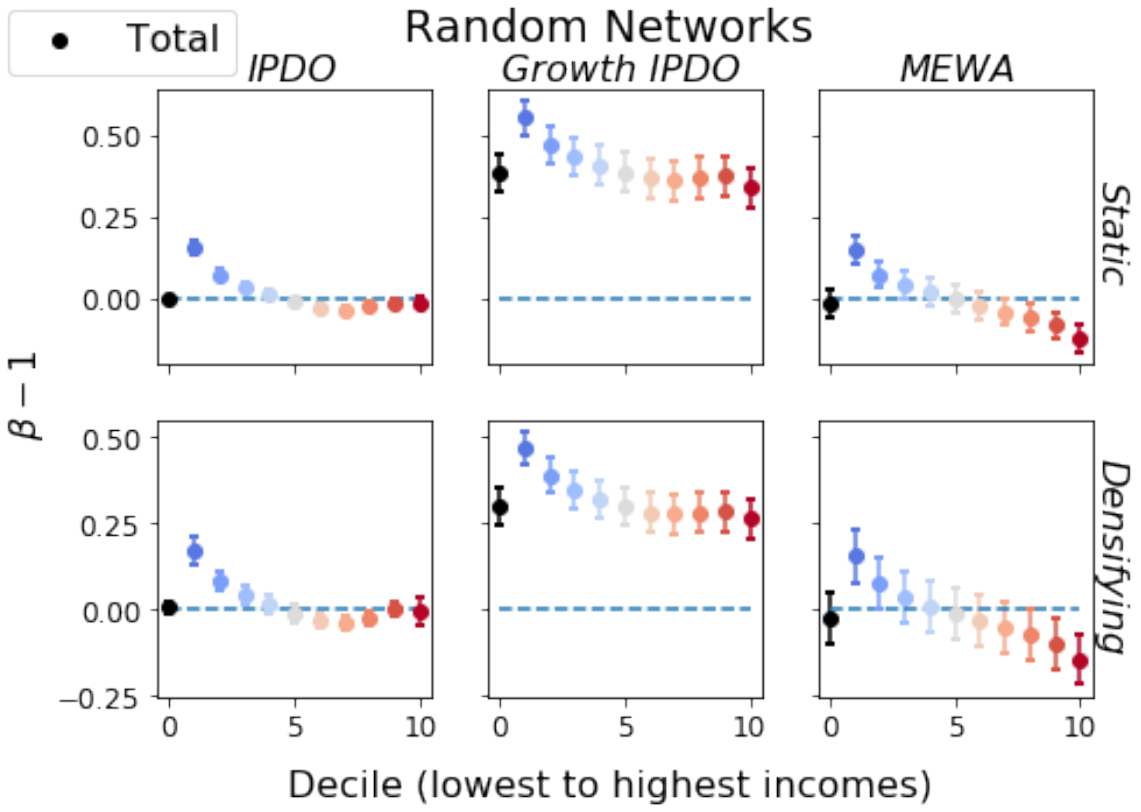

Figure (18) Decile scaling results for Kinetic Exchange Models ("IPDO": Equation 35, "Growth IPDO": Equation 37, "MEWA": Equation 39) on Random Networks ("Densifying": with increase in average number of edges per node over population size, "Static": with equal average number of edges per node). For each decile (1 through 10, with 10 being the highest-income earners), the scaling exponent is estimated within 95% confidence intervals. Figure 16 subfigure (c) serves as an empirical point of comparison. Surprisingly, a consistently *negative* relationship between β and decile is observed, which is opposite of the behavior observed empirically.

produce this effect are those on the scale-free network in Figure 20, though the relationship is not necessarily monotonically positive as it is in Figure 16.

It appears that what produces the positive β vs. n (decile) relationship observed in the Scale-Free networks (Figure 20) is network hubs. Network hubs—nodes (agents) with an exceptionally large number of neighbors—are characteristic of scale-free networks. In contrast, hubs are quite rare in small-world and random networks. The multiplicative exchange mechanism of all the simulated Kinetic Exchange Models creates dynamics that favor agents with more neighbors. An agent with many neighbors will split their exchange wealth evenly between its many neighbors, giving out only small amount to each neighbor, whereas agents with few neighbors will give larger amounts to their neighbors. A hub node connected to a node with few neighbors will benefit disproportionately from this edge. Because this is relatively common in the scale-free networks, many of these network hub nodes will acquire much larger wealth than their neighbors. Figure 21 shows this effect in

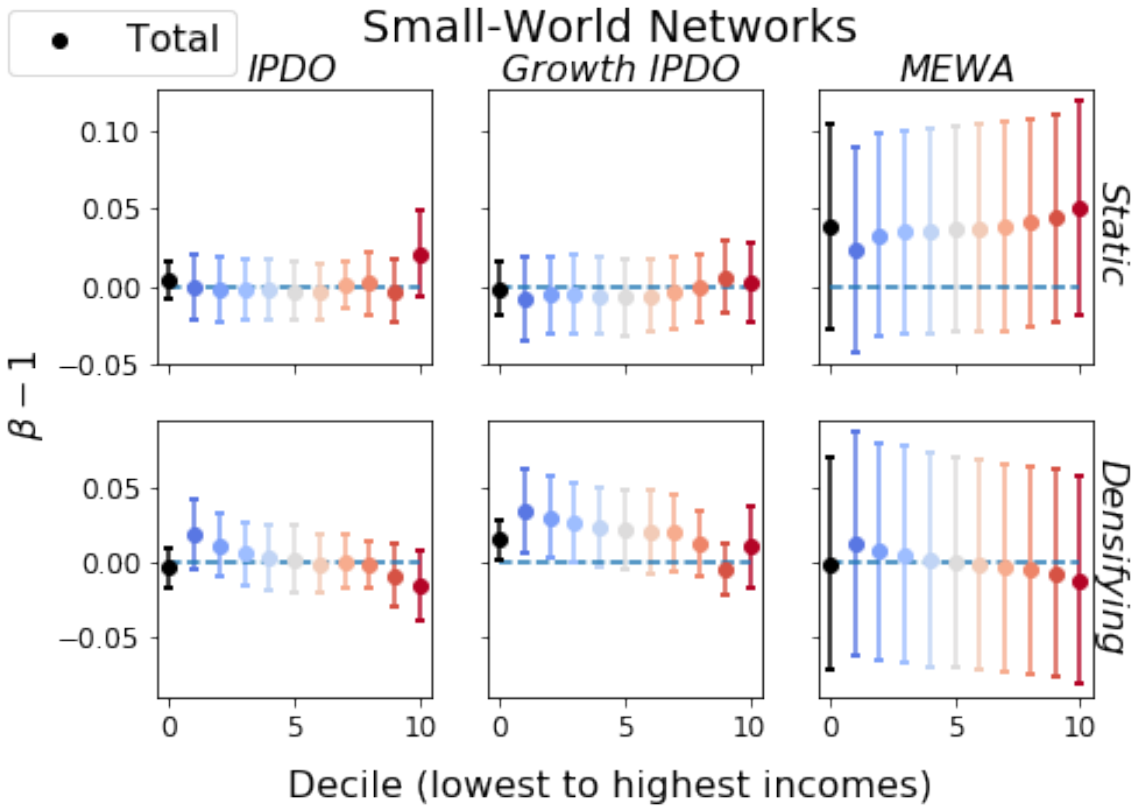

Figure (19) Decile scaling results for Kinetic Exchange Models ("IPDO": Equation 35, "Growth IPDO": Equation 37, "MEWA": Equation 39) on Small-World Networks ("Densifying": with increase in average number of edges per node over population size, "Static": with equal average number of edges per node). For each decile (1 through 10, with 10 being the highest-income earners), the scaling exponent is estimated within 95% confidence intervals. Figure 16 subfigure (c) serves as an empirical point of comparison. For most Small-World networks, deciles almost all exhibit approximately linear scaling and no clear trend between β and decile, though some show a negative trend, opposite of the empirical trend.

an IPDO run on a scale-free network: Agent wealth shows a clear relationship with nodal degree. The colormap of savings rates λ represents an already-observed effect of the IPDO: Agents with higher savings rates become more wealthy. The size-variance of this network hub effect is likely due to the existence of more network hub nodes in larger networks, though this needs further investigation.

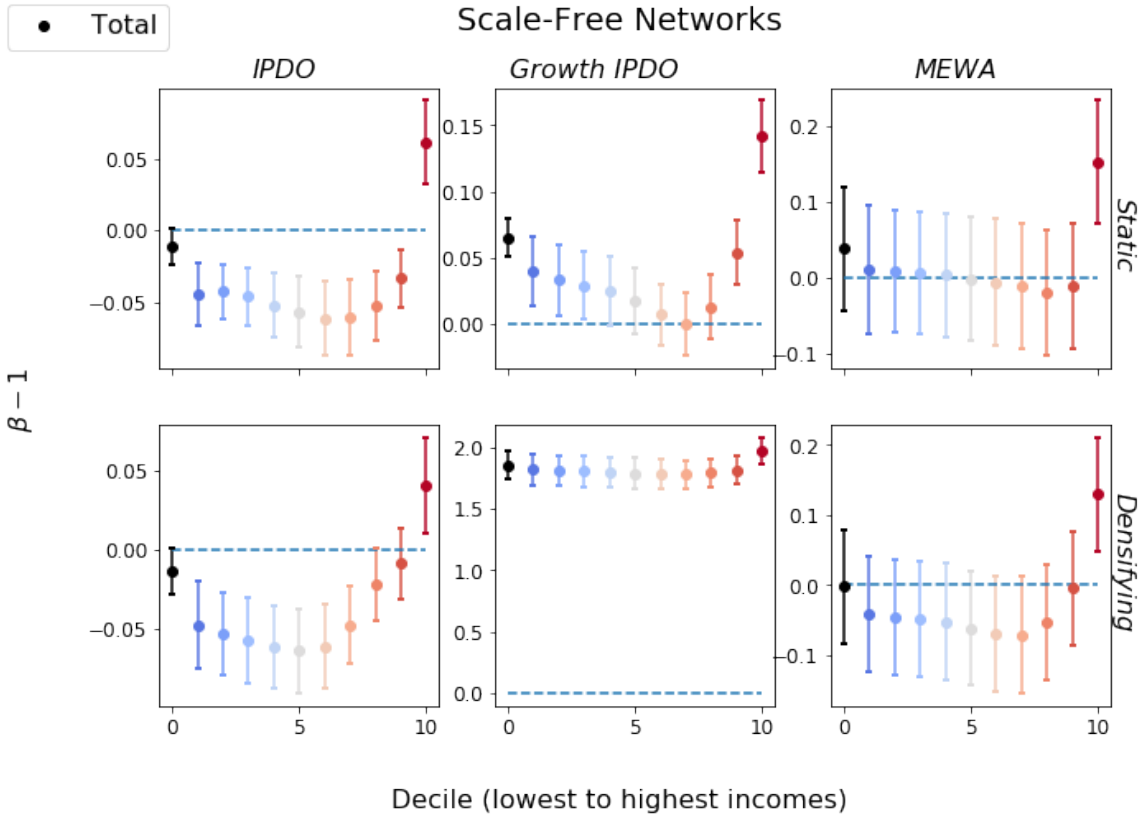

Figure (20) Decile Scaling Results for Kinetic Exchange Models ("IPDO": Equation 35, "Growth IPDO": Equation 37, "MEWA": Equation 39) on Scale-Free Networks ("Densifying": with increase in average number of edges per node over population size, "Static": with equal average number of edges per node). For each decile (1 through 10, with 10 being the highest-income earners), the scaling exponent is estimated within 95% confidence intervals. Figure 16 subfigure (c) serves as an empirical point of comparison. These results appear most similar to the empirical results in Figure 16, particularly the positive relationship between β and decile. However, the trend is not monotonically increasing as the empirical trend is. Instead, many results show only the top 10-30% of the population seeing more superlinear scaling.

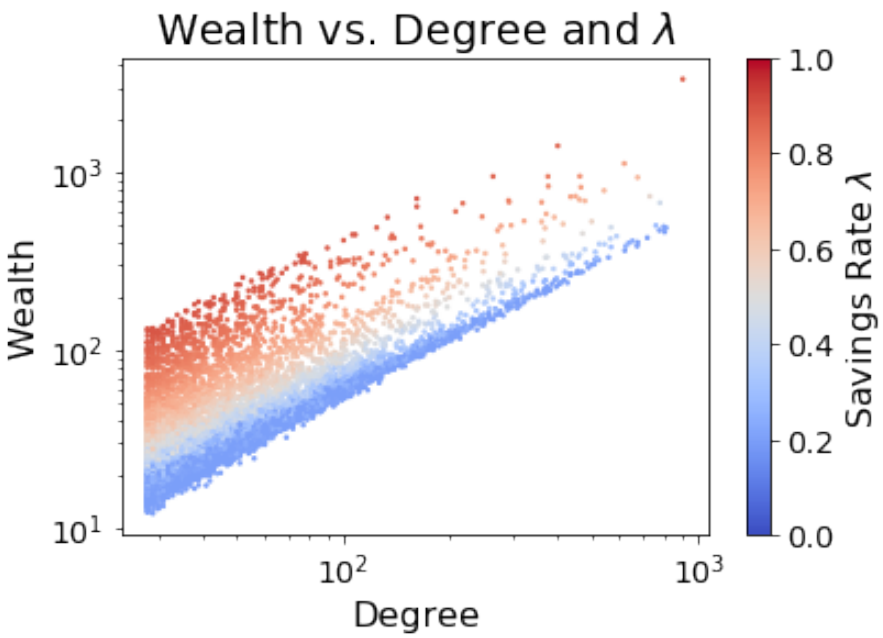

Figure (21) Relationship between agent wealth and the two agent characteristics that most drive wealth in the KEMs on a densifying scale-free network: Nodal degree (number of neighbors an agent has in the network) and savings rate λ. This shows a clear positive relationship between wealth and degree as well as between wealth and λ.

3.3 Conclusion & Discussion

In Section 3.1 we showed scaling inequality in US cities. Specifically, we added to a very new set of results in the urban scaling literature demonstrating urban allometry: different subpopulations within cities exhibiting different scaling behavior; in this study we only measure allometry of income. Our results align closely with those of Sarkar et al. [24, 25], though our methodology is slightly different producing slightly differing results. We also analyze the shape of these income distributions more rigorously as well as how these distributions change over city size. Our results indicate—within the urban scaling framework—that while cities scale income such that the total summed income grows per-capita in larger cities, certain subpopulations either do not experience this growth or in fact see negative growth (sublinear scaling) over city size. This is an important result for motivating future work investigating how other urban indicators are distribution *within* cities.

Additionally, in Section 3.2 we used Kinetic Exchange Modeling to explore potential causal mechanisms of the results observed in Section 3.1 based on urban scaling hypotheses. These results are very preliminary, but suggest that network structure may play a key role in producing the income inequalities observed in US cities which grows as cities get larger.

For future work, it would especially be interesting to investigate how the results of this section would compare with analyzing within-city distributions of other urban indicators such as crime rates. The hypothesis of urban scaling theory that urban outputs are outputs of social interactions suggests that different urban outputs should be characteristically similar

(e.g., all following a superlinear power-law of the population, Equation 1). Thus, if crime rates in neighborhoods within cities followed distributions similar to those for income (Figure 15, this would strongly support this city. Furthermore, it could have implications for understanding the size-variance of these distributions. Lastly, studies could be done to run different KEMs on different social network structures (perhaps derived empirically) to further investigate the effects seen in Section 3.2.

4 Discussion and Future Work

Together, the work in Chapters 2 and 3 extend Urban Scaling Theory to incorporate within-city and inter-city effects. Chapter 2 demonstrates a signification effect of inter-city networks, suggesting about 70% of urban outputs are attributable to local interactions while 30% are attributable to non-local or semi-local interactions. This challenges the implicit assumption of Urban Scaling Theory that cities are approximately isolated systems. We show that this is true to a "first-order" degree, but there may be important "second-order" effects of inter-city interactions, which may even be growing, though the time-variance is a topic for future study. In Chapter 2, we challenged the assumption of Urban Scaling Theory that cities contain homogeneous populations. We demonstrated empirically a scaling of inequality: higher-income sub-populations benefit disproportionately from urban agglomeration effects as compared to lower-income groups. We also were able to use Kinetic Exchange Modeling on social networks to prevent a possible causal mechanism for this empirical observation. Challenging these assumptions is intended not to attempt to delegitimize Urban Scaling Theory but to both extend its applications and test these applications to topics not yet analyzed within the urban scaling literature. Thus, this work both adds to urban scaling theory and connects it with research from Geography [20, 18], Sociology [11], and Economics [28].

The results in this thesis also prompt many avenues for further investigation. One of the potentially most fruitful possibilities is in connecting Chapter 2 and Chapter 3 to analyze how inter-city connectivities affect local income distributions. This could be carried about by merging some of the empirical analyses conducted here and/or by adapting the Kinetic Exchange Modeling to incorporate network edges between cities. Some studies have begun to explore these types of effects from other disciplines, though still none are connected to the urban scaling framework [21, 22]. Additionally, further work focused on specifically either inter-urban or intra-urban effects are warranted, though these possibilities are summarized in Sections 2.4 and 3.3.

We hope that these results motivate further investigations which merge urban scaling theory and observations with those of other disciplines related to Urban Science. Particularly, we believe that it is important that urban scaling literature continue the work done here to research urban allometry. The "economies of scale" frequently referenced in the agglomeration economics and urban scaling literature could in fact be "*dis*economies of scale," as we began to show in Section 3.1 by showing a scaling of income inequality across city size. This is greatly important in a world in which cities are becoming increasingly dominant in society and simultaneously inequality grows rapidly. We believe these avenues of investigation will not only strengthen the predictive power of Urban Scaling Theory but also make its

implications and predictions more relevant to policymakers. This is equally true for further understanding of inter-city effects, and further work connecting inter-city interactions with local income inequality is important to understanding how urban dynamics are shaping and being shaped by new social dynamics in today's world.

References

[1] Luís Ma Bettencourt, José Lobo, Dirk Helbing, Christian KÜhnert, and Geoffrey B West. Growth, Innovation, Scaling, and the Pace of Life in Cities. *Proceedings of the National Academy of Sciences*, 104(17):7301–7306, 2007.

[2] W Randall Haas Jr, Cynthia J Klink, Greg J Maggard, and Mark S Aldenderfer. Settlement-size Scaling Among Prehistoric Hunter-gatherer Settlement Systems in the New World. *Plos One*, 10(11):e0140127, 2015.

[3] Markus Schläpfer, Luís Ma Bettencourt, Sébastian Grauwin, Mathias Raschke, Rob Claxton, Zbigniew Smoreda, Geoffrey B West, and Carlo Ratti. The Scaling of Human Interactions With City Size. *journal of the Royal Society Interface*, 11(98):20130789, 2014.

[4] Luís Ma Bettencourt and José Lobo. Urban Scaling in Europe. *journal of the Royal Society Interface*, 13(116):20160005, 2016.

[5] James H Brown, James F Gillooly, Andrew P Allen, Van M Savage, and Geoffrey B West. Toward a Metabolic Theory of Ecology. *Ecology*, 85(7):1771–1789, 2004.

[6] Geoffrey B West, James H Brown, and Brian J Enquist. A General Model for the Origin of Allometric Scaling Laws in Biology. *Science*, 276(5309):122–126, 1997.

[7] Luís Ma Bettencourt. The Origins of Scaling in Cities. *Science*, 340(6139):1438–1441, 2013.

[8] Luís Ma Bettencourt, José Lobo, Deborah Strumsky, and Geoffrey B West. Urban Scaling and Its Deviations: Revealing the Structure of Wealth, Innovation and Crime Across Cities. *plos One*, 5(11):e13541, 2010.

[9] Peter J Taylor and Ben Derudder. *World City Network: a Global Urban Analysis*. Routledge, 2004.

[10] Thomas L Friedman. *The World is Flat: a Brief History of the Twenty-first Century*. Macmillan, 2005.

[11] Saskia sassen. *Global City*. Princeton University Press New York, London, Tokyo, 1994.

[12] United Nations. 2018 Revision of World Urbanization Prospects, 2018.

[13] Manuel Castells. Local and Global: Cities in the Network Society. *Tijdschrift Voor Economische en Sociale Geografie*, 93(5):548–558, 2002.

[14] Edward L Glaeser, Giacomo Am Ponzetto, and Yimei Zou. Urban Networks: Connecting Markets, People, and Ideas. *Papers in Regional Science*, 95(1):17–59, 2016.

[15] Peter J Taylor. Specification of the World City Network. *Geographical Analysis*, 33(2):181–194, 2001.

[16] Gilles Duranton and Diego Puga. Micro-foundations of Urban Agglomeration Economies. In *Handbook of Regional and Urban Economics*, volume 4, pages 2063–2117. elsevier, 2004.

[17] Diego Puga. The Magnitude and Causes of Agglomeration Economies. *journal of Regional Science*, 50(1):203–219, 2010.

[18] Evert J Meijers, Martijn J Burger, and Marloes M Hoogerbrugge. Borrowing Size in Networks of Cities: City Size, Network Connectivity and Metropolitan Functions in Europe. *Papers in Regional Science*, 95(1):181–198, 2016.

[19] Martijn J Burger and Evert J Meijers. Agglomerations and the Rise of Urban Network Externalities. *Papers in Regional Science*, 95(1):5–15, 2016.

[20] William Alonso. Urban Zero Population Growth. *Daedalus*, pages 191–206, 1973.

[21] Chunyang He, Yuanyuan Zhao, Jie Tian, and Peijun Shi. Modeling the Urban Landscape Dynamics in a Megalopolitan Cluster Area by Incorporating a Gravitational Field Model With Cellular Automata. *Landscape and Urban Planning*, 113:78–89, 2013.

[22] Michael Batty. Cities as Complex Systems: Scaling, Interaction, Networks, Dynamics and Urban Morphologies. 2009.

[23] Yanguang Chen and Linshan Huang. A Scaling Approach to Evaluating the Distance Exponent of the Urban Gravity Model. *Chaos, Solitons & Fractals*, 109:303–313, 2018.

[24] Somwrita Sarkar, Peter Phibbs, Roderick Simpson, and Sachin Wasnik. The Scaling of Income Distribution in Australia: Possible Relationships Between Urban Allometry, City Size, and Economic Inequality. *Environment and Planning B: Urban Analytics and City Science*, 45(4):603–622, 2018.

[25] Somwrita Sarkar. Urban Scaling and the Geographic Concentration of Inequalities by City Size. *Environment and Planning B: Urban Analytics and City Science*, 46(9):1627–1644, 2019.

[26] Kristian Behrens and Frédéric Robert Nicoud. Survival of the Fittest in Cities: Urbanisation and Inequality. *the Economic journal*, 124(581):1371–1400, 2014.

[27] Clémentine Cottineau, Olivier Finance, Erez Hatna, Elsa Arcaute, and Michael Batty. Defining Urban Agglomerations to Detect Agglomeration Economies. *arxiv Preprint Arxiv:1601.05664*, 2016.

[28] Nathaniel Baum Snow and Ronni Pavan. Inequality and City Size. *Review of Economics and Statistics*, 95(5):1535–1548, 2013.

[29] Raj Chetty, Nathaniel Hendren, and Lawrence F Katz. The Effects of Exposure to Better Neighborhoods on Children: New Evidence From the Moving to Opportunity Experiment. *American Economic Review*, 106(4):855–902, 2016.

[30] Nathan Eagle, Michael Macy, and Rob Claxton. Network Diversity and Economic Development. *Science*, 328(5981):1029–1031, 2010.

[31] Thomas Piketty. Capital in the 21st Century. 2014.

[32] Marc Barthelemy. The Statistical Physics of Cities. *Nature Reviews Physics*, 1(6):406–415, 2019.

[33] Claudio Castellano, Santo Fortunato, and Vittorio Loreto. Statistical Physics of Social Dynamics. *Reviews of Modern Physics*, 81(2):591, 2009.

[34] Mirta Galesic and Daniel L Stein. Statistical Physics Models of Belief Dynamics: Theory and Empirical Tests. *Physica a: Statistical Mechanics and Its Applications*, 519:275–294, 2019.

[35] Ilse Maria Fasol Boltzmann and Gerhard Ludwig Fasol. Ludwig Boltzmann (1844-1906). *Ludwig Boltzmann (1844-1906), Edited by Im Fasol-Boltzmann and Gl Fasol. Isbn 3-211-33140-9. Berlin: Springer, 2006.*, 2006.

[36] Bikas K Chakrabarti, Anirban Chakraborti, and Arnab Chatterjee. *Econophysics and Sociophysics: Trends and Perspectives*. John Wiley & Sons, 2006.

[37] Dov Monderer and Lloyd S Shapley. Potential Games. *Games and Economic Behavior*, 14(1):124–143, 1996.

[38] Victor M Yakovenko and J Barkley Rosser Jr. Colloquium: Statistical Mechanics of Money, Wealth, and Income. *Reviews of Modern Physics*, 81(4):1703, 2009.

[39] Vilfredo Pareto. *Cours D'économie Politique*, volume 1. Librairie Droz, 1964.

[40] Marco Patriarca, Els Heinsalu, and Anirban Chakraborti. Basic Kinetic Wealth-Exchange Models: Common Features and Open Problems. *The European Physical journal B*, 73(1):145–153, 2010.

[41] Anirban Chakraborti and Bikas K Chakrabarti. Statistical Mechanics of Money: How Saving Propensity Affects Its Distribution. *The European Physical journal B-Condensed Matter and Complex Systems*, 17(1):167–170, 2000.

[42] John Angle. The Inequality Process as a Wealth Maximizing Process. *Physica a: Statistical Mechanics and Its Applications*, 367:388–414, 2006.

[43] Thomas F Gieryn. A Space for Place in Sociology. *Annual Review of Sociology*, 26(1):463–496, 2000.

[44] Neil Brenner. Globalisation as Reterritorialisation: the Re-scaling of Urban Governance in the European Union. *Urban Studies*, 36(3):431–451, 1999.

[45] Robert E Kass and Adrian E Raftery. Bayes Factors. *journal of the American Statistical Association*, 90(430):773–795, 1995.

[46] Cate Heine, Chris Kempes, and Geoffrey West. Scaling and City Substructure. 2017.

[47] Arnab Chattejee. On Kinetic Asset Exchange Models and Beyond: Microeconomic Formulation, Trade Network, and All That. In *Mathematical Modeling of Collective Behavior in Socio-economic and Life Sciences*, pages 31–50. Springer, 2010.

[48] Alain Barrat and Martin Weigt. On the Properties of Small-World Network Models. *The European Physical journal B-Condensed Matter and Complex Systems*, 13(3):547–560, 2000.

[49] Albert-László Barabási and Eric Bonabeau. Scale-Free Networks. *Scientific American*, 288(5):60–69, 2003.

[50] Stanley Milgram. The Small World Problem. *Psychology Today*, 2(1):60–67, 1967.